Click Here for Full Article

Structure of the Maláguide Complex near Vélez Rubio (Eastern Betic Cordillera, SE Spain)

E. M. Fernández-Fernández,[1] A. Jabaloy-Sánchez,[1] F. Nieto,[2] and F. González-Lodeiro[1]

Received 6 July 2006; revised 7 February 2007; accepted 2 April 2007; published 25 July 2007.

[1] The Maláguide Complex of the Betic Cordillera represents a tectonic element which mostly underwent brittle deformation during the Alpine orogeny, and that covers the high-pressure/low-temperature (HP/LT) complexes of the internal Betic Cordillera. The evolution of this complex can help to determine both when the lower HP/LT complexes began to exhume and the behavior of the upper plate during this process. Moreover, this complex is a key element to understanding the relationships between the late orogenic extension in the internal Betic Cordillera and the coeval compression in the External Zones of the same mountain chain. This paper focuses in the geometry and kinematics of the Alpine structures of this Maláguide Complex in the eastern Betic Cordillera, near the village of Vélez Rubio. We propose that these Alpine structures can be grouped into three main stages. First stage (Paleogene) began with a synmetamorphic slaty cleavage produced in anchizone conditions. This foliation is associated with northward vergent structures and was probably connected with the superposition of the Maláguide Complex over the Alpujárride during the middle Eocene. This first stage ended with the thinning of the Maláguide Complex (Oligocene) by an extensional detachment with a top-to-the-NNW sense of movement. Second stage records the convergence of the External and Internal Zones during the Aquitanian-Burdigalian. This convergence was a right-lateral transpression that produced back thrusts and extensional structures that exhumed the HP/LT rocks of the Alpujárride Complex. Third stage corresponds to the evolution from the late Burdigalian to the present-day, when the Internal and External zones were welded together. **Citation:** Fernández-Fernández, E. M., A. Jabaloy-Sánchez, F. Nieto, and F. González-Lodeiro (2007), Structure of the Maláguide Complex near Vélez Rubio (Eastern Betic Cordillera, SE Spain), *Tectonics*, *26*, TC4008, doi:10.1029/2006TC002019.

[1]Departamento de Geodinámica, Universidad de Granada, Granada, Spain.
[2]Departamento de Mineralogía y Petrología, Universidad de Granada, Granada, Spain.

Copyright 2007 by the American Geophysical Union.
0278-7407/07/2006TC002019$12.00

1. Introduction

[2] The western Mediterranean area, comprising several basins with both continental and oceanic domains, formed from the Oligocene to the present-day. These basins are surrounded by Alpine mountain chains that developed mainly in the emerged areas of Africa and Europe, and also in the Corsica and Balearic Islands. Most of these mountain chains are coeval with the development of the basins. In the southern mountain belts of the western Mediterranean area (Betic, Rif, Tell, and Calabro-peloritans), there are several complexes that have undergone a metamorphic and deformation prior to the main orogenic stages of the mountain belt. These complexes of rocks have been usually called the Internal Zones in the Betic, Rif, and Tell. Most of the models of the evolution proposed for these belts imply a scenario wherein the Internal Zones complexes collided with a continental margin, thus triggering the orogeny. There is commonly a warn discussion among authors working in these areas concerning the identification and interpretation of the structures in these terranes, such as which structures predate the main orogenic event, which are coeval, and what kinematics and significance are (see, e.g., *Platt et al.* [2006] for a new interpretation of the whole evolution of the Betic Internal Zones).

[3] In the Betic-Rif Cordillera, *Balanyá and García Dueñas* [1987] defined the Alborán Domain (equivalent to the Internal Zones), which consists of allochthonous units. This Alborán Domain collided in the early Miocene with the rocks of the South Iberian Domain, which represents the ancient paleomargin of Iberia. Between the two domains are flysch units that form the Flysch Trough units. The rocks of the Alborán Domain can be grouped into three parts: the upper, mainly nonmetamorphic, Maláguide Complex, the intermediate Alpujárride Complex with Paleogene high-pressure/low-temperature (HP/LT) metamorphism [*Platt et al.*, 2005, 2006] and the lower Nevado-Filábride Complex with Neogene HP/LT metamorphism [*López-Sánchez-Vizcaíno et al.*, 2001; *Platt et al.*, 2006]. These rocks thrust over the South Iberian Domain rocks in the western and Central Betics [*Balanyá and García Dueñas*, 1987; *Balanyá*, 1991] with a top-to-the-NNW sense of movement [*Kirker and Platt*, 1998]. However, in the eastern Betic Cordillera, the South Iberian Domain rocks are superposed by a back thrust over the Alborán Domain with a top-to-the-SE sense of movement [*Paquet*, 1969; *Lonergan*, 1991, 1993] (Figure 1).

[4] The Maláguide Complex, which is the highest tectonic complex in the Alborán Domain of the Betic Cordillera, displays the most complete and best dated sequence in the entire Internal Zones, enabling relatively

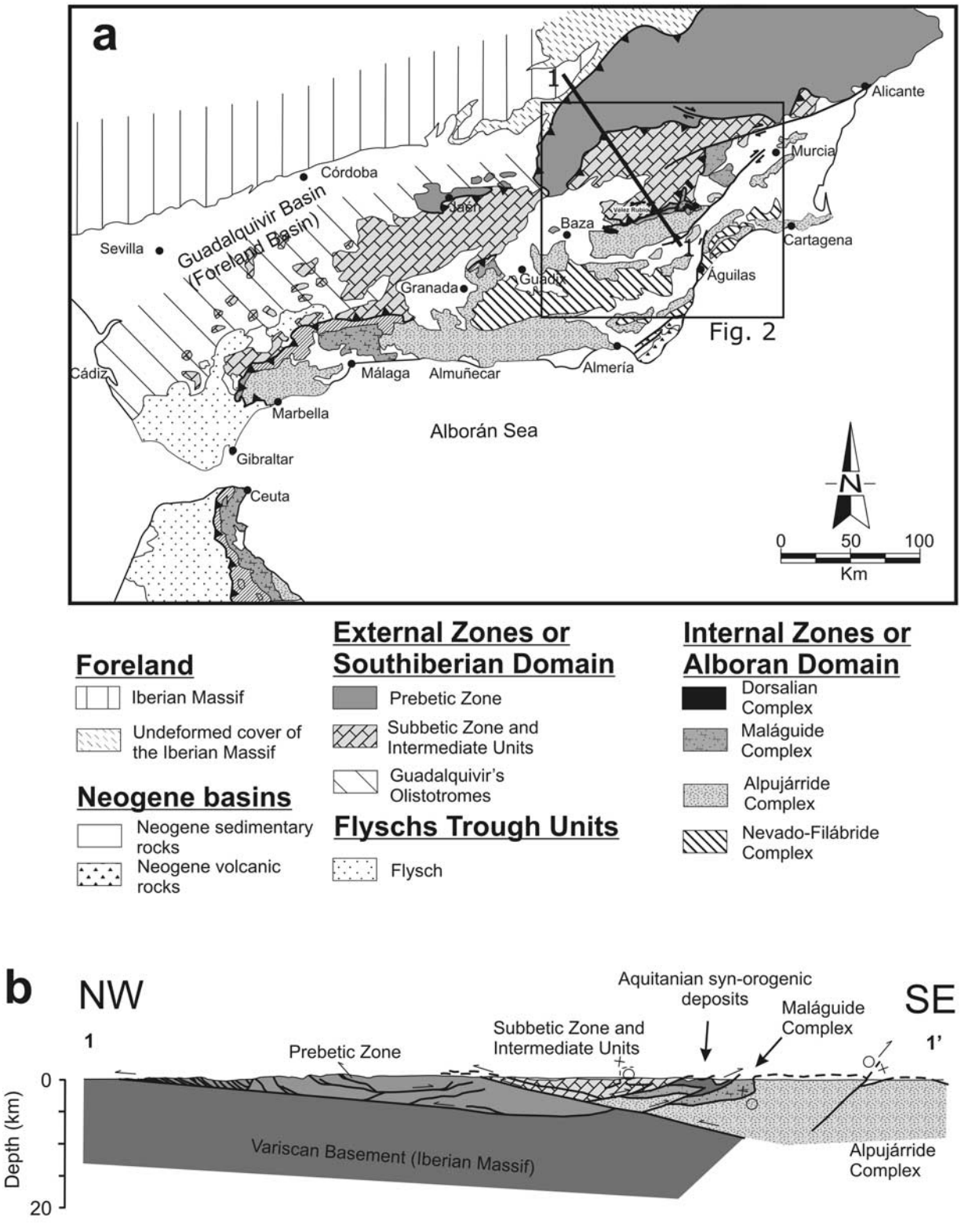

Figure 1. (a) Geological sketch of the Betic Cordillera and (b) cross section of the eastern sector of the mountain chain. The cross section was drawn using data from *Jabaloy-Sánchez et al.* [2007] and *Nebbad* [2001].

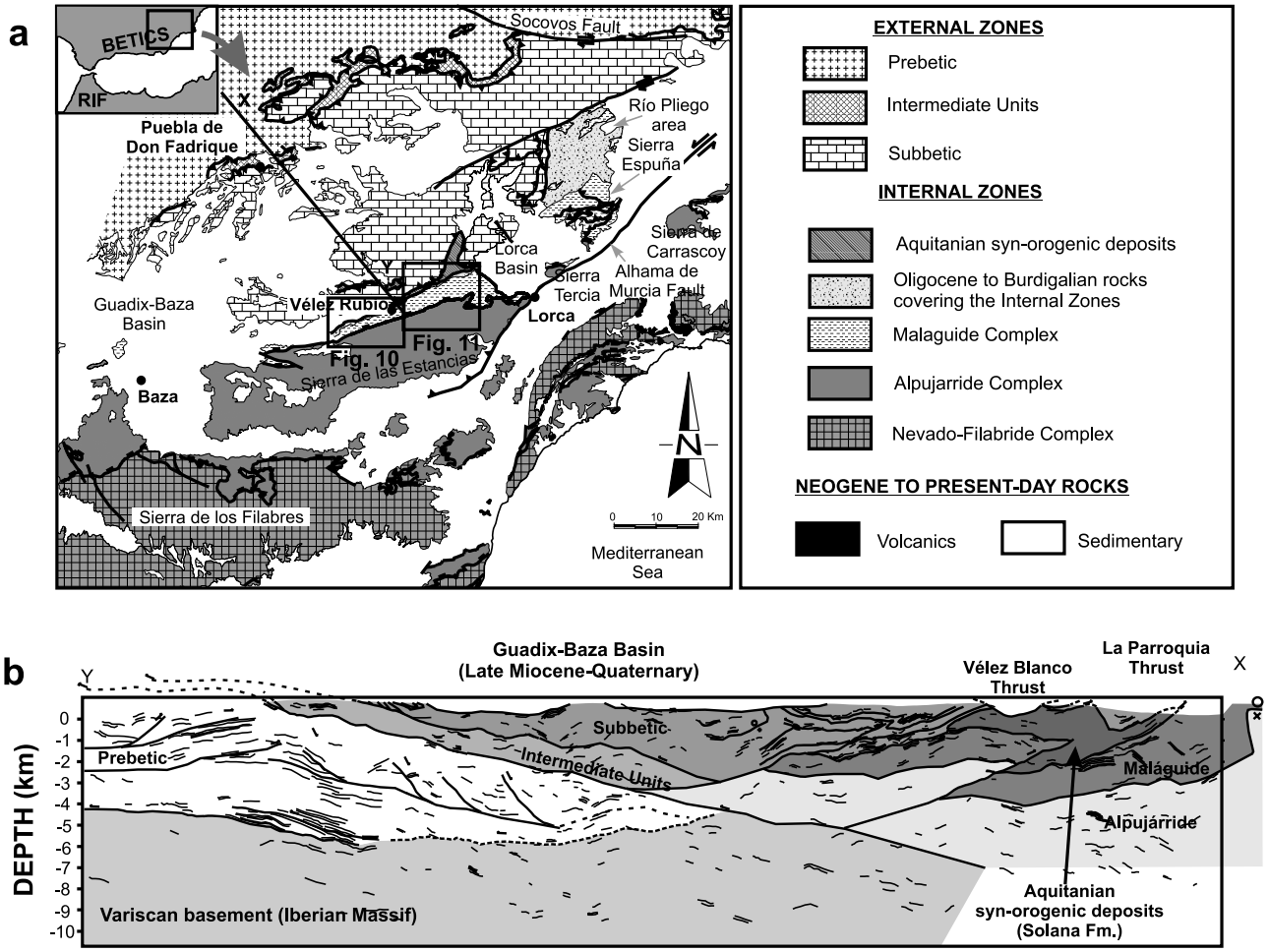

Figure 2. (a) Geological sketch of the eastern Betic Cordillera and (b) cross section of the upper curst of the area according to *Jabaloy-Sánchez et al.* [2007].

accurate dating of the structures. The sequence begins in the early Paleozoic and ends in the early Miocene. The outcrops that contain the most complete sequences are located in the eastern Betic Cordillera near the village of Vélez Rubio (Figures 1 and 2), whereas those in the western and central Betics usually lack the Jurassic to early Miocene rocks and the easternmost outcrops in the chain have practically no Paleozoic rocks. This area has been the subject of a number of field studies ever since 1960s [see *Lonergan and Platt*, 1995; *Geel and Roep*, 1998, and references therein] and their sedimentary sequence and lithological cartography are well established. Moreover, the area near Vélez Rubio shows the relationships of the complex with the South Iberian Domain rocks and with the HP/LT metamorphosed Alpujárride Complex and includes extensional structures such as low-angle normal faults and detachments [e.g., *Aldaya et al.*, 1991; *González-Lodeiro et al.*, 1996; *Lonergan and Platt*, 1995] and compressional structures such as thrusts and folds [*Paquet*, 1969; *Lonergan*, 1991, 1993].

[5] The main aim of this work is to present the structure of the Maláguide Complex in the area of Vélez Rubio. This will aid in determining the structures that predate the major convergence between the Alborán and the South Iberian domains, those that are coeval to this convergence, and those that postdate it. We have also established the kinematics of these structures, their mutual relationships, and their relationships with the synorogenic deposits. We have then focused on the evolution of the Alboran Domain and the mechanisms of the exhumation of the HP-LT complexes below the Maláguide Complex.

2. Geological Setting

[6] The Betic Cordillera extends south and eastward in the Iberian Peninsula. Within the orogen, two major zones have been recognized: the Internal Zones [*Fallot*, 1948], or Alborán Domain [*Balanyá and García Dueñas*, 1987], and the External Zones [*Fallot*, 1948], or South Iberian Domain [*Balanyá and García Dueñas*, 1987]. The rocks of the Internal Zones have usually undergone Alpine metamorphism, while those of the External Zones are sedimentary rocks deposited in the southern and eastern margin of the

Iberian Massif. In the western part of the chain, the two zones are separated by the turbiditic deposits of the Flysch Trough Units (Figure 1).

[7] In the eastern Betic Cordillera (Figures 1 and 2), from north to south, the following structures can be identified in the External Zones: (1) the fold-and-thrust belt of the Prebetic, which developed over a wedge of sedimentary rocks with shallow marine and paralic facies; (2) the thrust of the Intermediate Units formed by a sequence of Cretaceous pelagic rocks where Jurassic deposits are omitted; and (3) the pop-up structure of the Subbetic bounded by two divergent thrust surfaces.

[8] In the Vélez Rubio area, the rocks of the Subbetic underwent compressive deformation during the Burdigalian [*Fernández-Fernández et al.*, 2004]. The first deformations recorded in these rocks are a trend of approximately N-S folds verging east (early Burdigalian) that were tightened and affected by vertical axis rotations during the middle Burdigalian [*Fernández-Fernández et al.*, 2004]. These rocks thrust over the Solana Formation (attributed to the Aquitanian) with a SE sense of movement of the hanging wall, and the thrust surface was eroded and covered by upper Burdigalian deposits [*Fernández-Fernández et al.*, 2004].

[9] In the area around Vélez Rubio, between the Internal and the External Zones, lies a body of green and brown marls with quartzitic sandstones and calcarenites called the Solana Formation. Some authors correlate this formation with the Flysch Trough Units [*Martín-Algarra*, 1987], although we interpret it as part of the synorogenic deposits associated with the convergence between the two zones [*Jabaloy-Sánchez et al.*, 2007]. The rocks of the Solana Formation thrust over the rocks of the Maláguide Complex, probably during the upper Burdigalian [*Fernández-Fernández et al.*, 2004], with a top-to-the-SE sense of movement.

[10] The Internal Zones of the eastern Betic Cordillera contain the three main complexes defined in the chain: the Nevado-Filábride, Alpujárride and Maláguide [*Egeler and Simon*, 1969] (Figures 1 and 2), which are superposed in the aforementioned order. The present-day contacts of these complexes in this traverse are extensional detachments and low-angle normal faults [e.g., *Aldaya et al.*, 1991; *Galindo-Zaldívar et al.*, 1989; *Jabaloy et al.*, 1993; *Lonergan and Platt*, 1995]. The Maláguide is well represented in this traverse by four main outcrops: the area of Vélez Rubio to the west, Sierra Tercia and Sierra Espuña in the center, and Sierra de Carrascoy to the east (Figure 2). The extensional detachment associated with the Alpujárride-Maláguide contact has an ENE sense of movement of the hanging wall [*Aldaya et al.*, 1991; *Lonergan and Platt*, 1995]. The cooling ages of the footwall, the Alpujárride Complex, obtained by fission track studies in apatites and zircons, suggest an age between 21 and 18 Ma for the movement of this detachment [*Johnson*, 1993; *Platt et al.*, 2005].

[11] *Lonergan* [1991, 1993] has recognized several deformation stages during the evolution of the Maláguide Complex in Sierra Espuña. The first stage, during the late Eocene and Oligocene, produced thrusts with a N-NW sense of movement of the hanging wall. The second stage, during the middle Burdigalian, corresponds to the thrusting of the Subbetic over the Internal Zones. All these structures were subsequently folded with NW vergence during the middle Miocene.

3. Description of the Rocks of the Maláguide Complex

3.1. Sedimentary Sequence

[12] The sedimentary sequence of the Maláguide Complex in the study area has a basement composed of Paleozoic rocks (Late Silurian to Late Carboniferous) deformed and metamorphosed into greenschist facies during the Variscan orogeny (Figures 3 and 4). The rocks of this basement are called the Piar Group, and in the western Betic Cordillera can include Ordovician and older rocks. This basement is overlain by a Mesozoic-Paleogene cover that is normally detached in the study area (Figures 3 and 4). The cover begins with the red mudstones, sandstones and conglomerates, with some interlayered levels of dolostones and gypsum, of the Saladilla Formation (middle late Triassic) [*Simon and Visscher*, 1983; *Kozur et al.*, 1985; *Mäkel and Rondeel*, 1979; *Mäkel*, 1985]. In the eastern part of the study area, this formation is metamorphosed and the mudstones evolve to red and violet slates. This mainly detritic formation is overlain by the limestones and dolostones of the Castillón, Vélez Rubio and Xiquena Formations, with ages ranging from Jurassic to early Eocene (Figures 3 and 4).

[13] This succession is covered by detritic Neogene formations. The lowest detritic Neogene formation is the Ciudad Granada Formation, which lies unconformably over the lower rocks of the sequence. It consists of yellow, brown and reddish brown calcarenites, sandstones and mudstones containing clasts from the lower Maláguide formations [*Mac Gillavry et al.*, 1963; *Geel*, 1973; *Hermes*, 1977]. Thickness is extremely variable, ranging from 180–200 m in the west [*González Donoso et al.*, 1988] to 5 m near Vélez Rubio and La Parroquia [*Geel*, 1973]; its age is early middle Aquitanian [*González Donoso et al.*, 1988] (Figure 3). The formation begins with shallow marine gravitational deposits that evolve toward pelagic facies [*Soediono*, 1971; *Geel*, 1973], indicating significant tectonic subsidence in the Maláguide [*Geel and Roep*, 1998].

[14] The Maláguide sequence ends with the Fuente-Espejos Formation, which has an early Burdigalian to lower part of the late Burdigalian age [*González Donoso et al.*, 1988; *Geel and Roep*, 1998] (Figure 3). This formation is unconformably over the aforementioned rocks and comprises gray-green marls with levels of calcarenites, sandstones, breccias and conglomerates showing signs of mass transport. These rocks contain clasts from the Maláguide and Alpujárride complexes, and the upper part of the sequence also includes clasts from the Subbetic and the Solana Formation [*Geel*, 1973; *Geel and Roep*, 1998]. In the study area occurrences of the late Eocene-Oligocene rocks described eastward in the Sierra Espuña and Rio Pliego areas by *Paquet* [1969], *Lonergan* [1993], and *Martín-Martín et al.* [1996] are lacking.

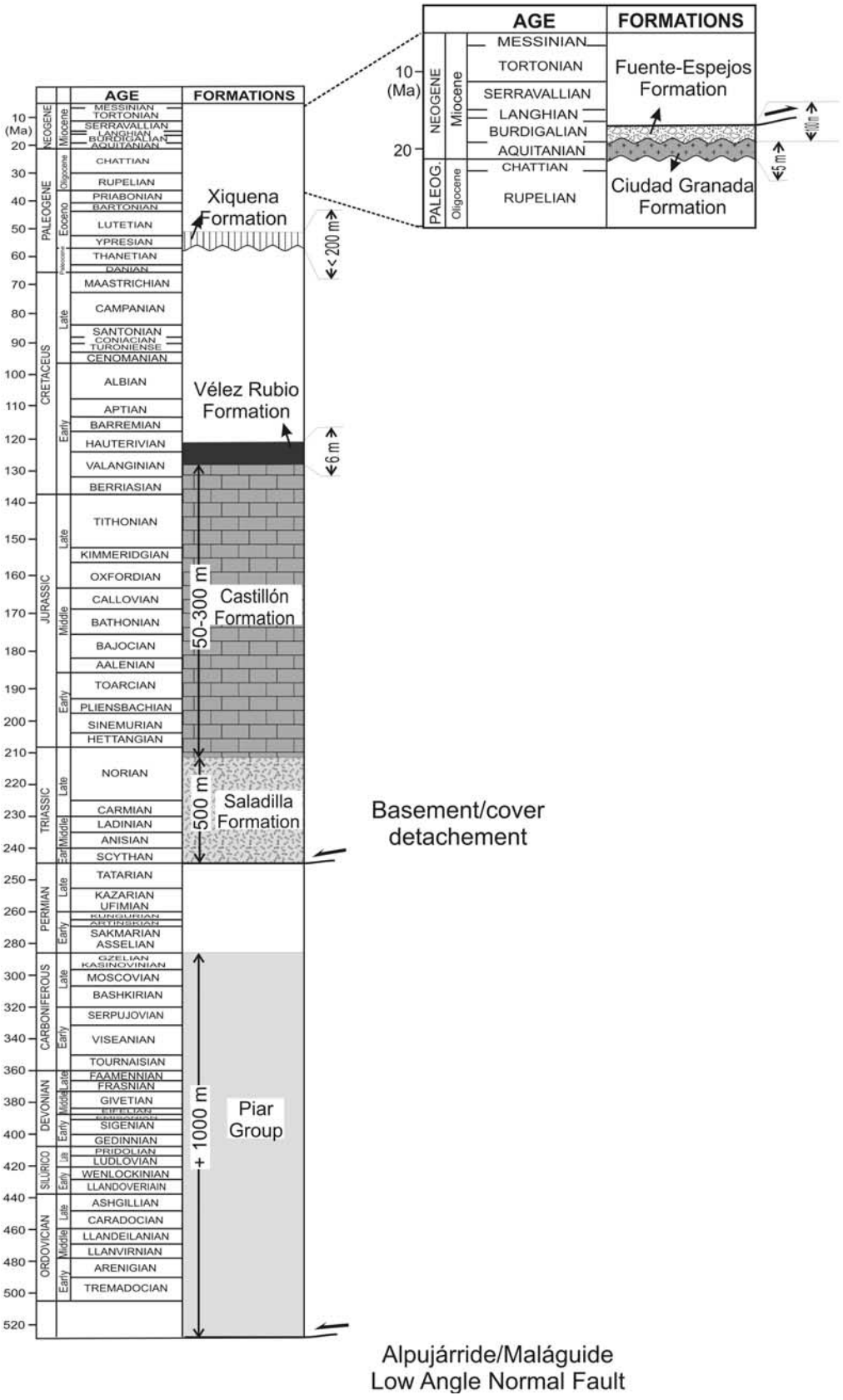

Figure 3. Lithological column of the Maláguide Complex in the area near Vélez Rubio. The major detachment faults (thick lines) and unconformities (undulated lines) are marked.

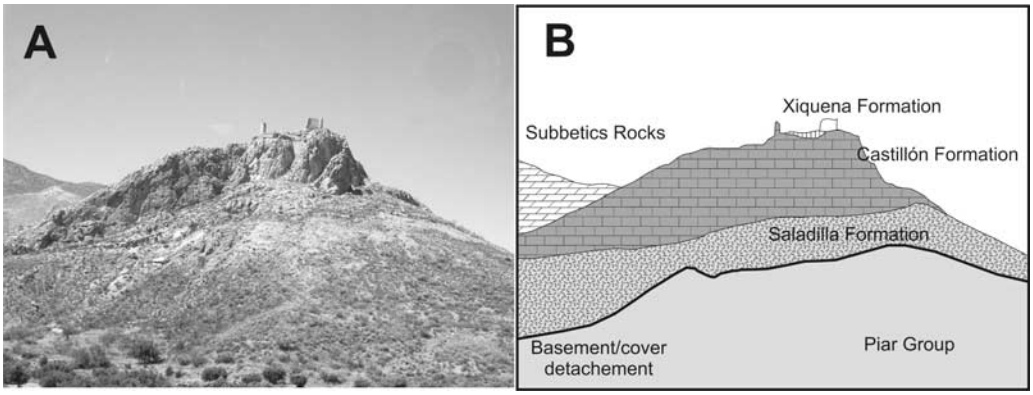

Figure 4. (a) View of the Xiquena Castle, east of Vélez Rubio village, where nearly the whole lithological sequence of the Maláguide Complex outcrops, and (b) line drawing interpretation of Figure 4a.

3.2. Intrusive Basalts

[15] The studied area commonly contains dikes of basic igneous rocks intruding both the Maláguide and Alpujárride complexes. These dikes crosscut the bedding of the Piar Group in the nonmetamorphic units of the upper Maláguide; also they cut the bedding and the synmetamorphic Alpine slaty cleavage when intruding into the Middle to Upper Triassic rocks of the Saladilla Formation in the lower metamorphic Maláguide units (Figure 5). Moreover, they cut the main foliation within the Alpujárride phyllites. They vary in thickness from 1 to 1.5 m, have N-S and E-W strikes and are usually subvertical (Figure 6).

[16] The rocks are "basalts" with ophitic textures and plagioclase, pyroxene, amphiboles, and opaques as the primary mineral association. These minerals are replaced by calcite, quartz, chlorite, and epidotes (including allanite). The presence of chlorite indicates a low-temperature metamorphic event after their intrusion because, in mafic rocks, the phyllosilicates that are stable at low temperatures (usually under 200°C) are smectites or mixed layers clay minerals and chlorite (usually between 200°C and 230°C), whereas chlorite is the dominant mafic phyllosilicate for temperatures higher than 240°C [*Bevins et al.*, 1989]. A similar low-temperature metamorphic event has been described by *Duggen et al.* [2004] in the dikes swarm and surrounding host rocks of the Málaga region in the western Betic Cordillera. The fact that this metamorphic imprint can be recognized in all the basalts whenever they have intruded: (1) in the nonmetamorphic upper Maláguide, (2) the anchizonal metamorphic lower Maláguide, and (3) the epizonal (with HP/LT conditions) Alpujárride rocks suggest that this imprint is later than the intrusion and the metamorphism in the host rocks. The fact that this metamorphism also produces calcite indicates that the whole composition of the rocks is not conserved and that this metamorphism is probably associated with secondary hydrothermal alteration.

[17] The sampled rocks are mainly subalkaline basalts and basaltic andesites (Figure 6). The alteration has affected the major element composition and Si, Fe, Mg, Ca, Na and K have probably been remobilized during the secondary hydrothermal alteration and very low grade metamorphism. Therefore we have classified these samples using the less mobile elements.

[18] The samples represented in the Hf-Th-Ta discrimination diagram after *Wood* [1980] displays mainly between the fields of the mid-ocean ridge basalt (MORB), island arc tholeiites and calc-alkali basalts and the field of the volcanic arc basalts (Figure 7). The same samples in the Ti/Zr discrimination diagram after *Pearce and Cann* [1973] and in the Ti/Zr/Y discrimination diagram after *Pearce and Cann* [1973] locate within the field of the MORB, island arc tholeiites and calc-alkali basalts (Figure 7). All these diagrams allow us to classify the samples as island arc tholeiitic basalts in agreement with the classification of similar intrusive basalts in the Málaga region studied by *Torres-Roldán et al.* [1986], *Turner et al.* [1999], and *Duggen et al.* [2004].

[19] The mantle and the normal MORB (NMORB) normalized patterns of the trace elements of the samples (Table 1 and Figure 7) indicate a relative enrichment in incompatible trace elements: Rb, Ba, Th, U, Sr and Ti, while they are

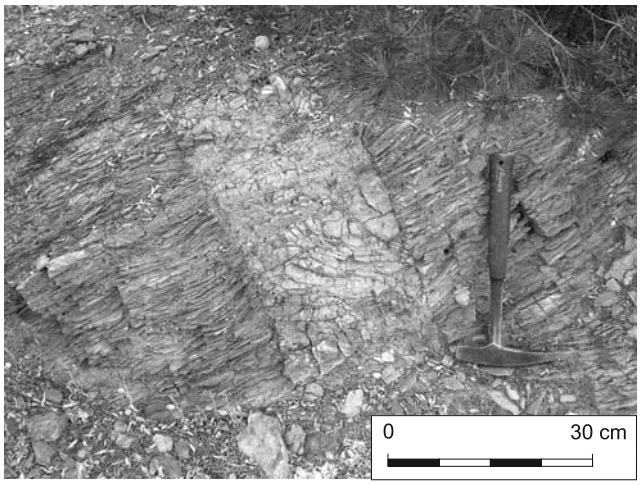

Figure 5. A dike of basalt cutting the violet foliated pelites of the Middle-Upper Triassic Saladilla Formation.

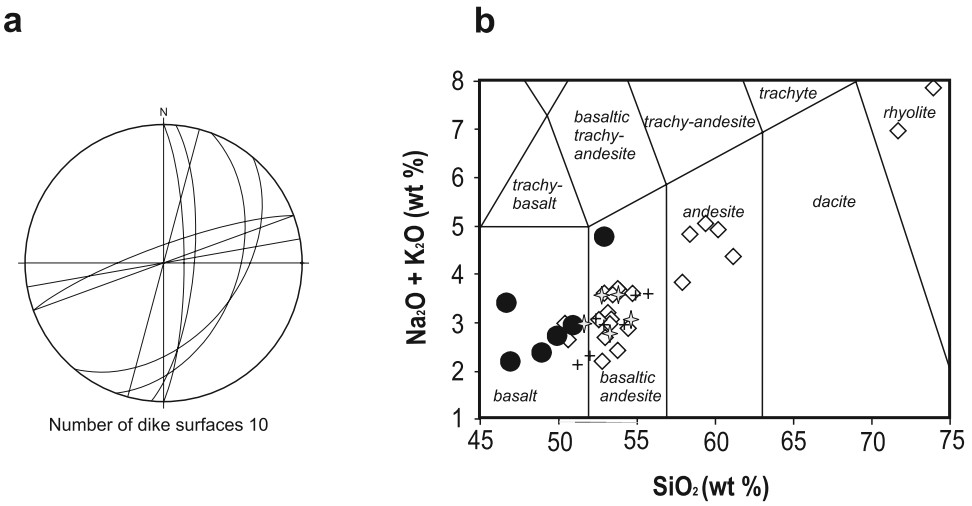

Figure 6. (a) Stereogram with the orientation of the wall surfaces of the dikes in both the Maláguide and Alpujárride complexes and (b) total alkali-silica diagram [after *Le Bas et al.*, 1986] for the analyzed samples (solid circles) and those samples near Málaga studied by *Torres-Roldán et al.* [1986] (crosses), *Turner et al.* [1999] (stars), and *Duggen et al.* [2004] (diamonds).

slightly depleted in the light rare earth elements (Figure 7). In this respect, they are similar to those reported by *Turner et al.* [1999] and *Duggen et al.* [2004].

[20] Rare earth elements show rectilinear and flat chondrite normalized patterns, coincident with those commonly reported for mid-ocean ridge basalts (MORB) and island arc tholeiites (IAT), and there are no negative Eu anomalies, which indicate the absence of plagioclase fractionation (Figure 7).

[21] In order to clarify the existence or not of a contribution from an upper continental crust derived material we have used the Th/Nb versus La/Nb diagram [*Plank*, 2005]. In this diagram our samples, together with the samples from *Turner et al.* [1999] and *Duggen et al.* [2004], define a linear plot like those defined by the samples of other island arc basalts: e.g., Antillas Arc and not within the MORB-oceanic island basalt (OIB), thus suggesting an island arc affinity (Figure 8). The Th/Nb versus La/Nb diagram also include the isopleths of the Th/La ratio, which is generally greater in the arc setting than in the abyssal lavas and is mainly influenced by the composition of the subducted sediments [*Plank*, 2005]. The samples have a high Th/La ratio (around the line of Th/La = 0.3) (Figure 8) as those of the material from the upper continental crust, thereby indicating a contribution of upper continental crust rocks to the upper mantle.

[22] All the available ages from these dikes are obtained in the western traverse of the chain, as there are none in the study area. The age proposed for the intrusion ranges between 37.6 ± 0.9 Ma (whole rock $^{40}Ar/^{39}Ar$ step-heating age determined by *Turner et al.* [1999]) and 33.6 ± 0.6 Ma (laser $^{40}Ar/^{39}Ar$ on a plagioclase from a basalt, determined by *Duggen et al.* [2004]). Younger ages have also been determined in the matrix of the dikes and in the whole rocks. These younger ages vary between 17.7 ± 0.6 and 19.1 ± 0.4 Ma [*Turner et al.*, 1999], between 17.4 ± 0.4 and 19.8 ± 1.0 Ma [*Duggen et al.*, 2004] for the matrix analyses, and between 22 and 23 Ma for the whole rock K-Ar ages [*Torres-Roldán et al.*, 1986]. *Duggen et al.* [2004] propose that the younger ages correspond with the age of the thermal overprint of the dikes and the host rocks that may correspond with the hydrothermal alteration and very low grade metamorphism in the area.

4. The Structure of the Maláguide Complex

4.1. Paleogene Alpine structures

[23] The oldest Alpine structure recognized in the Maláguide Complex in the study area is a slaty cleavage (Figure 9). This slaty cleavage develops in the pelitic rocks of the Piar

Figure 7. Representation of the analyzed samples (solid circles) and those samples near Málaga studied by *Torres-Roldán et al.* [1986] (crosses), *Turner et al.* [1999] (stars), and *Duggen et al.* [2004] (diamonds) in several discrimination diagrams using the less mobile elements and the trace elements patterns of the igneous rocks. (a) Hf-Th-Ta discrimination diagram after *Wood* [1980]. A, field of the NMORB; B, field of the MORB; island arc tholeiites and calc-alkali basalts; C, field of the alkaline within-plate basalts; and D, field of the volcanic arc basalts. (b) the Ti/Zr discrimination diagram after *Pearce and Cann* [1973]. A, field of the island arc tholeiites; B, MORB, island arc tholeiites, and calc-alkali basalts; C, field of the calc-alkali basalts; and D, MORB. (c) Ti/Zr/Y discrimination diagram after *Pearce and Cann* [1973]. A, field of the island arc tholeiites; B, field of the MORB, island arc tholeiites and calc-alkali basalts; C, field of the calc-alkali basalts; and D, within-plate basalts. (d) Trace element concentrations normalized to the composition of NMORB. (e) Trace element concentrations normalized to the composition of chondrite. (f) Trace element concentrations normalized to the composition of the primitive, mantle fields of the Caribbean Early Cretaceous IAT (gray area) from *Blein et al.* [2003 and references therein].

Group (Paleozoic) and the Saladilla Formation (Middle-Upper Triassic), although only in the lower rocks of the eastern part of the area (Figures 10 and 11). This foliation, whose surfaces are usually subhorizontal, is axial planar to folds with N80°E to E-W trending hinges and vergences toward the north. This structure has also been described in the lower Maláguide units of Sierra Espuña [*Lonergan*, 1991; *Nieto et al.*, 1994] and of Sierra Tercia [*Booth Rea*, 2001].

[24] The cleavage is planar and penetrative in thin section in the pelites, but is not well developed in the sandstones or conglomerates. In the pelites with quartz, the cleavage domains anastomose around the detritic quartz grains. Most of the slates have a phyllitic shine in the cleavage surfaces. The cleavage domains are composed by the metamorphic phyllosilicates, usually the phengites, paragonites, chlorites and/or pyrophyllite.

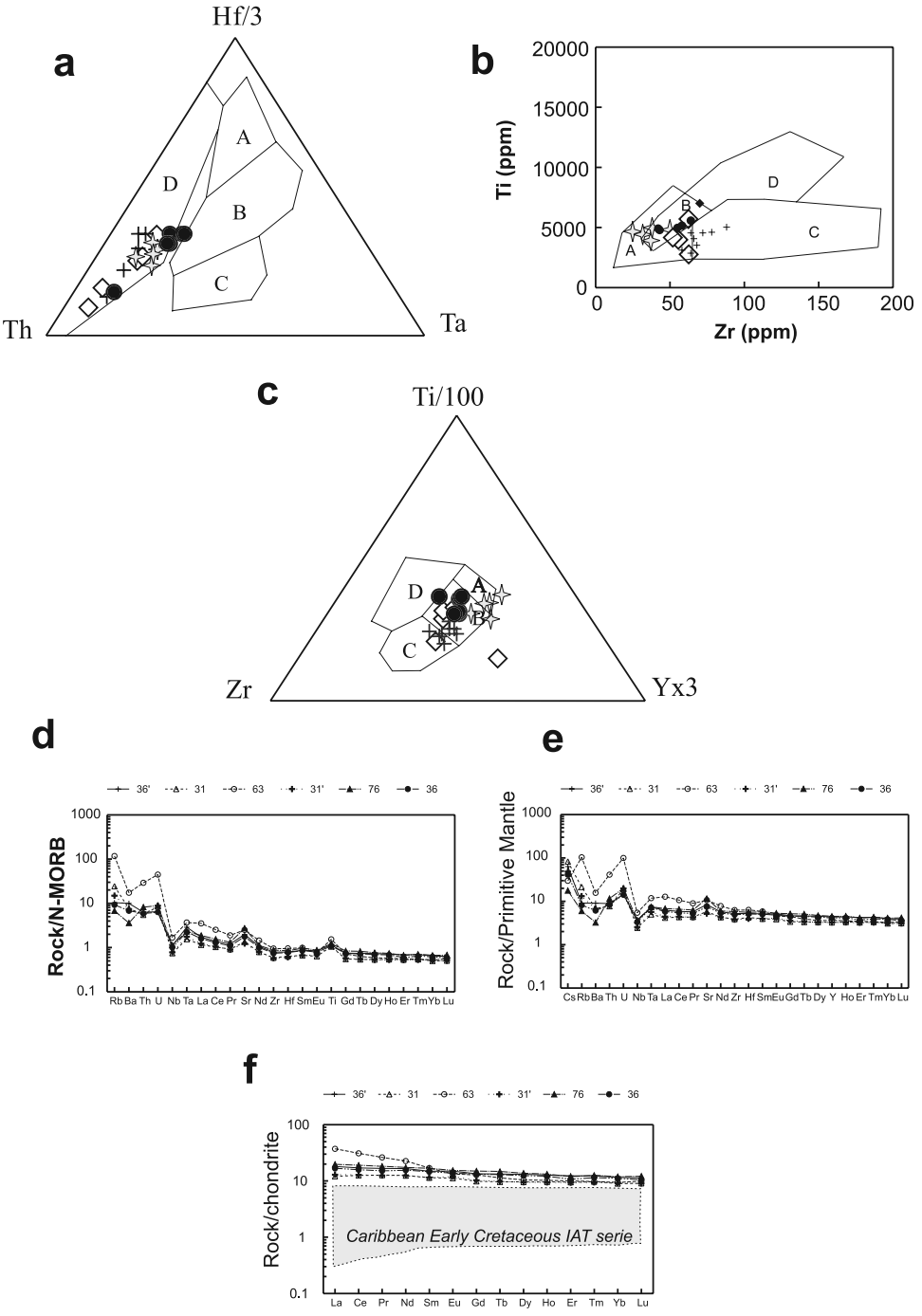

Figure 7

Table 1. Composition of the Basalts in Major and Trace Elements[a]

	Sample					
	36′	31	63	31′	76	36
Latitude	37°40′22″N	37°40′13″N	37°37′17″N	37°40′13″N	37°41′06″N	37°40′22″N
Longitude	1°53′54″W	1°55′15″W	2°05′15″W	1°55′15″W	1°53′01″W	1°53′54″W
SiO_2, wt%	51.08	47.53	53.86	47.54	49.94	50.03
Al_2O_3	16.45	14.53	16.09	14.52	15.43	15.77
Fe_2O_3	8.86	9.08	7.79	9.11	9.17	8.67
MnO	0.15	0.15	0.12	0.14	0.16	0.14
MgO	6.69	4.85	4.10	4.89	5.42	6.54
CaO	10.57	10.29	6.28	10.3	10.5	11.78
Na_2O	2.82	1.98	3.12	1.89	2.33	2.61
K_2O	0.12	0.16	1.65	0.3	0.04	0.11
TiO_2	0.86	0.8	1.17	0.82	0.93	0.83
P_2O_5	0.08	0.06	0.11	0.07	0.1	0.07
LOI	1.8	10.27	6.01	10.06	6.37	3.25
Rb, ppm	5.781	13.641	65.816	8.374	3.813	5.175
Cs	2.032	2.648	0.954	1.554	0.565	1.320
Sr	178.390	121.548	225.753	110.722	245.572	158.735
Ba	63.168	48.074	109.727	46.704	22.644	42.759
Y	19.805	14.851	16.741	14.878	20.571	18.848
Nb	2.590	1.739	3.892	1.821	2.644	2.357
Ta	0.302	0.204	0.486	0.233	0.306	0.297
Zr	58.517	43.554	70.384	42.521	64.539	55.226
Hf	1.619	1.311	1.963	1.229	1.729	1.588
U	0.305	0.397	2.1	0.415	0.42	0.298
Th	0.754	0.657	3.502	0.692	0.986	0.711
La	4.278	2.871	8.812	3.065	4.679	3.968
Ce	10.424	7.703	18.919	7.865	11.626	9.663
Pr	1.581	1.207	2.49	1.186	1.732	1.437
Nd	7.739	5.802	10.552	5.882	8.098	7.248
Sm	2.28	1.75	2.591	1.766	2.558	2.227
Eu	0.866	0.65	0.772	0.69	0.89	0.8
Gd	2.761	2.022	2.631	2.111	3.079	2.719
Tb	0.497	0.361	0.424	0.367	0.551	0.483
Dy	3.341	2.436	2.638	2.404	3.478	3.169
Ho	0.718	0.546	0.579	0.534	0.748	0.686
Er	2.036	1.572	1.660	1.546	1.983	1.778
Tm	0.316	0.247	0.249	0.24	0.321	0.292
Yb	1.973	1.524	1.604	1.572	2.031	1.887
Lu	0.288	0.231	0.253	0.229	0.31	0.265

[a]Samples 36′, 31, 31′, 76 and 36 come from the Maláguide Complex, and sample 63 comes from the Alpujárride Complex.

[25] We have taken several samples of red pelites from the Saladilla Formation (Figure 11 and Table 2) in order to establish the conditions during this deformation. The samples were studied by X-ray diffraction (XRD) in order to determine mineral assemblages and the conditions of metamorphism. Samples were washed and homogeneous rock chips were used for preparation for XRD. Whole rock samples and clay fractions (<2 μm) were analyzed using a Philips PW 1710 powder diffractometer with Cu-Kα radiation, graphite monochromator and automatic divergence slit. The <2 μm fraction was separated by repeated extraction of supernatant liquid subsequent to settling. Oriented aggregates were prepared by sedimentation on glass slides. Ethylene-glycol (EG) treatment was carried out on all the samples in order to corroborate the identification of smectite and/or illite-smectite mixed layers. Preparations of samples and experimental conditions for illite ''crystallinity'' (Kubler Index, KI) measurements were carried out according to IGCP 294 IC Working Group recommendations [*Kisch*, 1991b]. The KI values were measured from the <2 μm fractions, <2 μm EG-treated fractions, and for the bulk rock samples. These KI values (y) can be transformed into CIS values (x) according to the equation y = 0.5247x + 0.00604 (r = 0.998), obtained in the laboratory using the international standards of *Warr and Rice* [1994].

[26] On the basis of XRD results, two different groups of samples can be identified (Table 2). The first group includes samples LP-1, LP-2, LP-3, and LP-7, and the second group includes samples LP-4, LP-6, LP-10, and LP-16. They can be differentiated based on their mineral composition and Kubler indices (KI). The first group is characterized by abundant kaolinite, an absence of pyrophyllite and paragonite, and KI indices ranging from 0.57 to 0.65° 2θ. In the second group, kaolinite is absent, paragonite or pyrophyllite present, and KI ranges from 0.35 to 0.52° 2θ. All the samples show clear differences between KI measured on air-dried and ethylene-glycol treated samples, which allows us to identify the presence of small amounts of R3 illite/smectite mixed layers (I/S) giving an XRD peak superposed

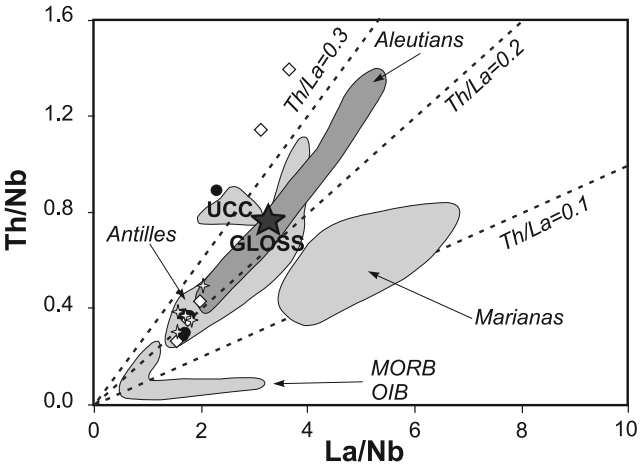

Figure 8. Th/Nb versus La/Nb plots for igneous rocks from the analyzed samples (solid circles) and those samples near Málaga studied by: *Turner et al.* [1999] (stars) and *Duggen et al.* [2004] (diamonds). Fields of MORB-OIB, Marianas, Aleutians, Antilles arcs, upper continental crust (UCC), and global subducting sediment (GLOSS, star) from *Plank* [2005, and references therein].

on the mica 10 Å peak. The effect of this peak, together with that at 9.6 Å, corresponding to paragonite, on the 10 Å first peak of mica prevents the normal use of the latter to establish metamorphic grade. Therefore KI has also been measured on the 5 Å second peak of mica, which produces equivalent results to the first one but is free of significant effects from I/S and paragonite [*Nieto and Sánchez-Navas*, 1994; *Battaglia et al.*, 2003]. When KI is measured on this peak, the first group of samples presents values between 0.43 and 0.50° 2θ, corresponding to deep burial diagenetic conditions. The values of the second group range between 0.32 and 0.38° 2θ, that is, anchizone conditions, which is in perfect agreement with the presence of pyrophyllite and paragonite in the samples. In addition, the KI of whole rock samples has been measured to check for detrital mica. In general this parameter presents lower values than those measured in the <2 μm fraction, indicating a moderate presence of detrital mica; however, in many cases the difference is slight. All the samples contain quartz and mica, and usually hematite as well, which produces the characteristic red coloring. Chlorite is present in some samples from both groups. The samples in the first group lack slaty cleavage, whereas those in the second group have visible slaty cleavage. This lack or presence of slaty cleavage in the rocks coincides with the deformation and metamorphic conditions deduced from the mineral composition and KI. Moreover, this occurrence or lack also agrees with the observations of the development of the slaty cleavage at very low grade conditions recompiled by *Kisch* [1989] and discussed by *Kisch* [1991a].

[27] Kaolinite is a typical sedimentary mineral, transformed at the onset of metamorphism. In contrast, paragonite and pyrophyllite are characteristic very low and low-grade metamorphic minerals, frequently described in the anchizone and epizone [*Frey*, 1987]. Under conditions where water pressure equals lithostatic pressure ($a_{H2O} = 1$), the presence of pyrophyllite indicates temperatures above 300°C; however, in nature, water activity can be expected to be less than unity. *Frey* [1987] estimated 270°C at the kaolinite + quartz → pyrophyllite reaction isograd of the external zone of the central Swiss Alps.

[28] The minor presence of I/S in all the samples can be ascribed to retrograde diagenesis [*Nieto et al.*, 2005]. This process was first described in the Maláguide Complex in Sierra Espuña by *Nieto et al.* [1994] and later corroborated in a varied set of sequences of different ages and geological conditions. The Maláguide rocks in the Velez Rubio area are clearly more affected by retrograde diagenesis than those in Sierra Espuña, where the alteration process affects only chlorite in some samples. Nevertheless, the metamorphic character of the second group of samples is clearly demonstrated by pyrophyllite and paragonite, which are index metamorphic minerals, thermodynamically incompatible with I/S. These retrograde conditions may be correlated with the hydrothermal overprint detected in the basalts within the dike swarm that *Duggen et al.* [2004] dated as early Miocene.

[29] There is no clear age for this slaty cleavage due to the lack of radiometric dating, although *Lonergan* [1993] associated it with the Eocene-Oligocene thrust system in the Maláguide of Sierra Espuña. Furthermore, the swarm of basalt dikes dated as upper Eocene [*Turner et al.*, 1999; *Duggen et al.*, 2004] cut this foliation and we therefore tentatively propose a middle Eocene age for this structure.

[30] These island arc tholeiitic basalt dikes, cutting both Alpujárride and Maláguide rocks, mainly strike N-S and E-W with subvertical dips that are usually parallel to the joint sets in the host rocks. The dikes cut the slaty cleavage in the Saladilla Formation (Figure 5) and also the main metamorphic foliation within the Alpujárride rocks. Below the Maláguide Complex, the Alpujárride dominant rocks are blue phyllites with a metamorphic foliation that is defined by white mica. These phyllites contain carpholite pseudomorphs, suggesting PT conditions around 300°C and 7 kbar [*Goffé et al.*, 1989, *Martínez-Martínez and Azañón*, 1997]. The $^{40}Ar/^{39}Ar$ ages of the white micas of the foliation of this

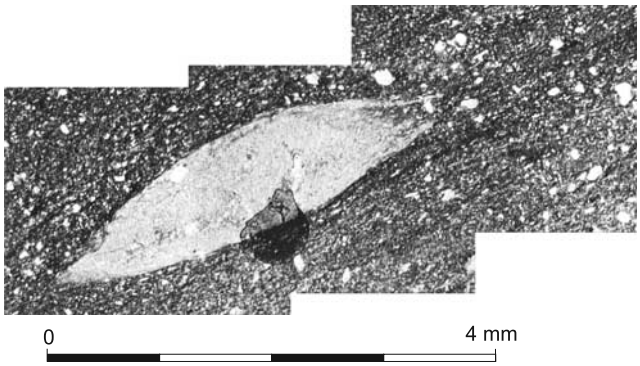

Figure 9. Photography of the slaty cleavage developed in the Middle-Upper Triassic Saladilla Formation (photomosaic obtained by combining a series of micrographs).

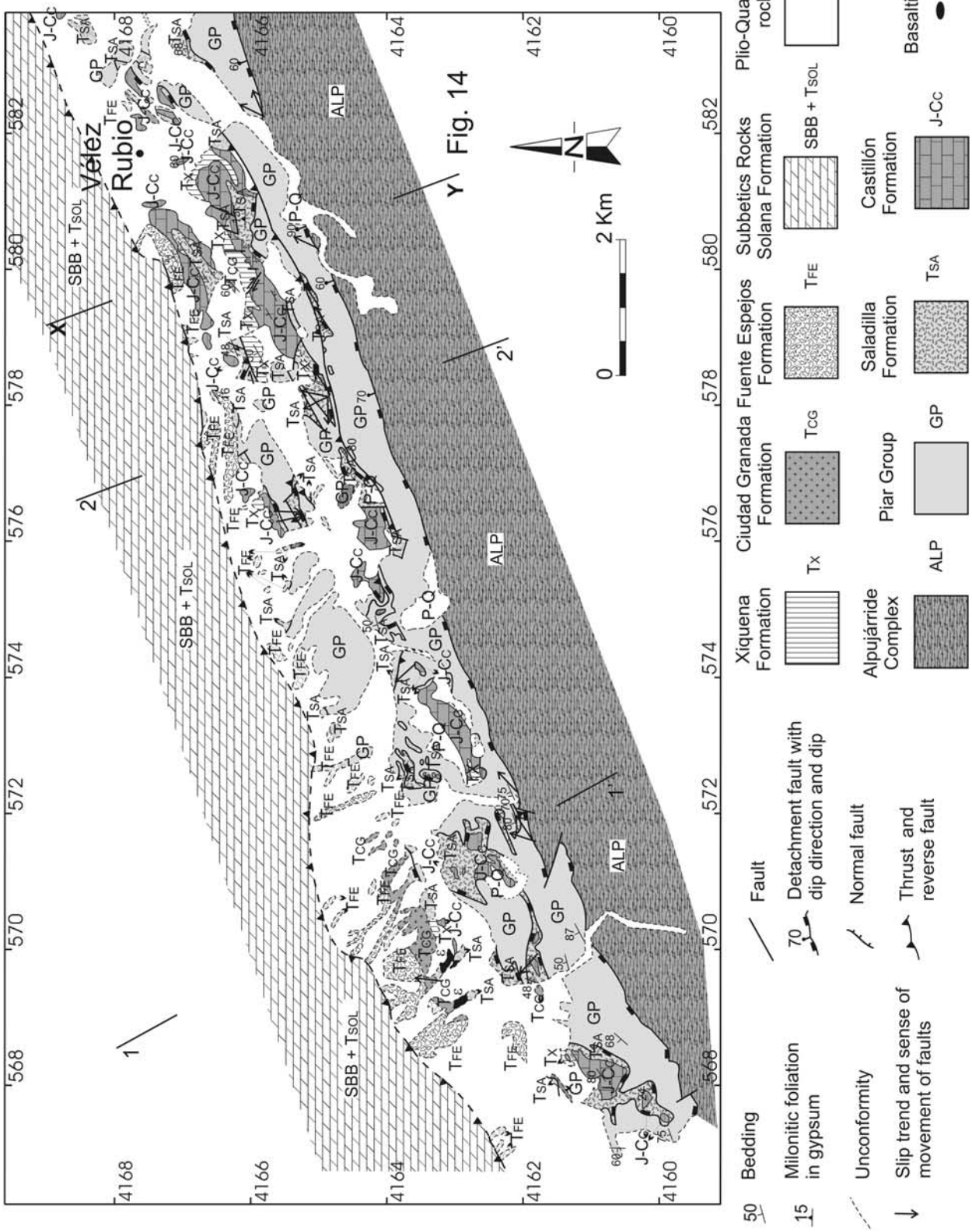

Figure 10. Geological map of the Maláguide Complex west of Vélez Rubio village. See Figure 2 for location.

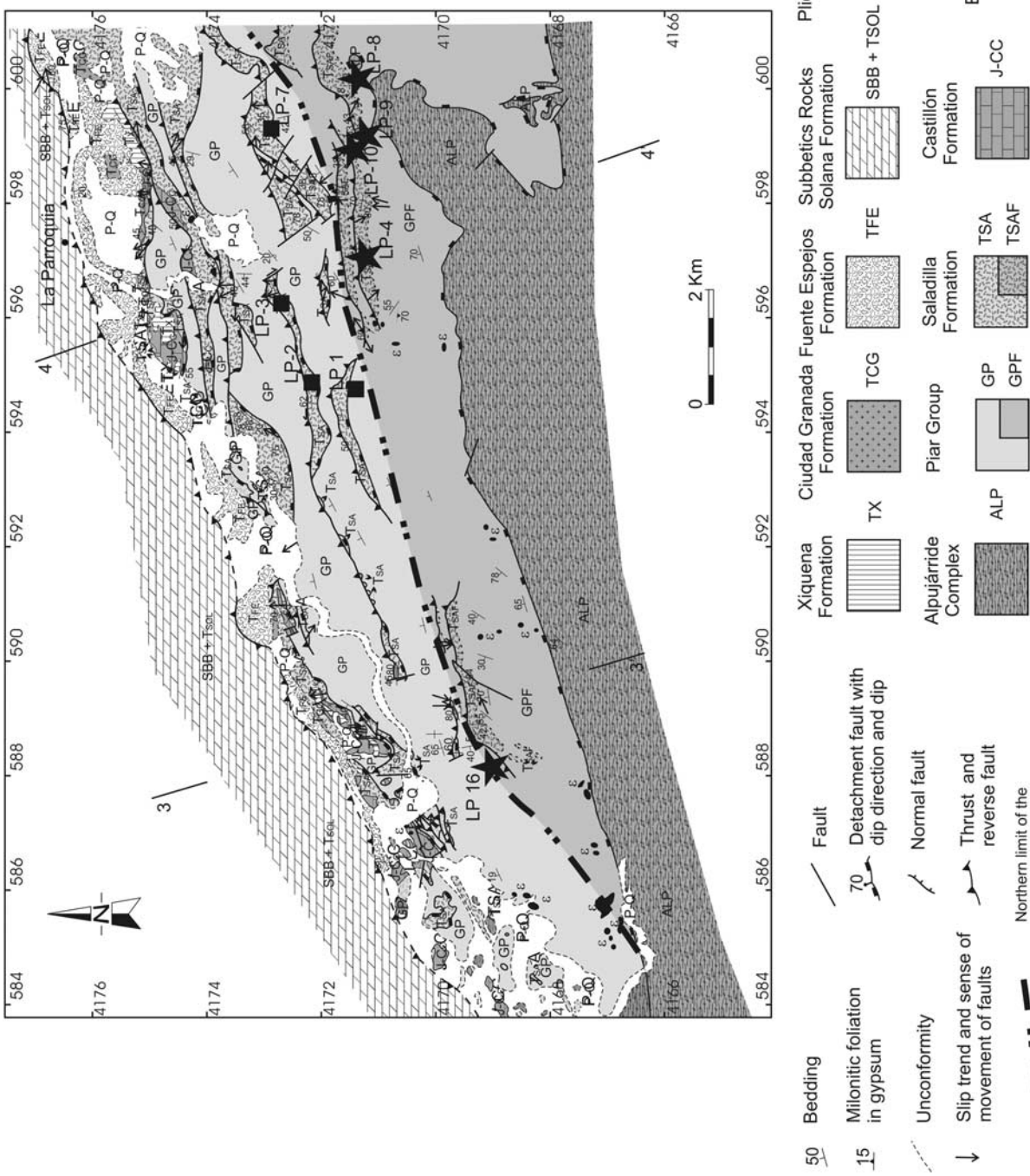

Figure 11. Geological map of the Maláguide Complex east of Vélez Rubio village. The area with the development of the Alpine foliation is marked and also the location of the samples of Table 2 (star, anchizone; solid square, diagenesis). See Figure 2 for location.

Table 2. Illite "Crystallinity" Kubler Index[a]

Sample	Minerals	10 Å			5 Å		b	d_{001} cta	d_{001} mica	Conditions
		<2μ	EG	Total	<2μ	Total				
Lp 1	quartz, mica, chlorite	0.57	0.74	0.61	0.46	0.35	8.987	14.16	9.986	diagenesis
Lp 2	quartz, mica, hematite, kaolinite	0.65	0.60	0.53	0.43	0.41		—	9.992	diagenesis
Lp 3	quartz, mica, hematite, kaolinite	0.62	0.64	0.60	0.44	0.31		—	9.992	diagenesis
Lp 4	quartz, mica, pyrophyllite, chlorite	0.45	0.44	0.39	0.37	0.26	8.987	14.14	10.000	anchizone
Lp 7	quartz, mica, hematite, kaolinite	0.58	0.52	0.52	0.50	0.31		—	9.988	diagenesis
Lp 8	quartz, mica, chlorite, hematite, paragonite	0.36	0.41	0.41	0.32	0.32	9.001	14.16	9.987	anchizone
LP 9	quartz, mica, chlorite, hematite, paragonite	0.45		0.37	0.34	0.25		14.17	9.990	anchizone
Lp 10	quartz, mica, pyrophyllite	0.35	0.45	0.36	0.33	0.28	8.982	—	9.999	anchizone
Lp 16	quartz, mica, chlorite, hematite, pyrophyllite	0.52	0.51	0.49	0.38	0.29	8.986	14.16	9.988	anchizone

[a]Measurements are from the <2 μm fractions and <2 μm EG-treated fractions and for the bulk rock samples (in the 10 Å peak) and from the <2 μm fractions and for the bulk rock samples (in the 5 Å peak) of the micas in the pelites from the Saladilla Formation (Middle-Late Triassic). See text for discussion.

rocks determined by *Platt et al.* [2005] indicate an age of 48 Ma for the formation of this fabric. The dikes, then, are clearly later than 48 Ma (early Eocene). In addition, the ages established by *Turner et al.* [1999] and *Duggen et al.* [2004] for this swarm in the western Betic Cordillera are late Eocene to early Oligocene. Consequently, we too propose a late Eocene to early Oligocene age for these basalts in the eastern Betic Cordillera.

[31] The fault zone detaching the Mesozoic-Cenozoic cover from the Paleozoic basement is one of the older structures formed during the Alpine orogeny in the Vélez Rubio region (Figures 10, 11, and 12). This fault zone is observed only in the areas where the Triassic rocks of the Saladilla Formation display no slaty cleavage. The faults strike N70°E to N80°E and dip 30° to 70° toward the NNW (Figures 10, 11, and 12). This high-angle dip is due to the late folding. The late folding is ENE-WSW antiform with a vertical limb that produces the tilting of the ancient structures.

[32] The fault zone does not contain mylonites or cohesive cataclasites but rather contains uncohesive fault rocks. The transition from the fault rocks to the unfractured rocks is sharp and the fault zone is several meters thick in the whole area and is formed by incoherent fault gouges and fault breccias (see definition of these terms in the work by *Snoke and Tullis* [1998]) that contain numerous microfaults. Most of these microfaults are parallel to the main fault zones and are arranged as brittle S-C structures. These microfault surfaces contain striae with a NNW-SSE trend, and the kinematic criteria within the gouge zone (S-C structures and crushed tails on clasts) indicate a NNW sense of movement of the hanging wall (Figure 13). Within these surfaces, there is also a second set of ENE-WSW trending striae that is less abundant than the NNW-SSE set. This ENE-WSW set has associated right- and left-lateral senses of movement. Moreover, there are microfault surfaces with NNW-SSE strikes that act as tear faults within the fault rock (Figure 13). The second set of ENE-WSW trending striae with right- and left-lateral senses of movement seems to record a later deformation superposed on the NNW-SSE trend; this set of ENE-WSW striae is subparallel to the striation in the Maláguide/Alpujárride detachment fault described in the next section.

[33] This fault surface, with its NNW sense of movement of the hanging wall, is discontinuous in the cartography because it is intersected and displaced by a set of reverse faults (Figures 10, 11, and 12). In the central splays, the fault zone separates the Saladilla Formation (Middle-Late Triassic) from the Piar Group (Paleozoic). However, in the northern splays, the fault surface thins and omits the Triassic Saladilla Formation and the Jurassic to lower Eocene Castillón and Xiquena Formations directly overlie the Paleozoic Piar Group (Figure 14). Rocks of the Ciudad Granada Formation (early-middle Aquitanian) cap this fault surface.

[34] The present-day discontinuous nature of this fault zone makes it difficult to reconstruct the original geometry. If we unfold the NNW vergent folds and take into account the movement of the Neogene reverse faults, the fault seems to correspond to a single fault surface. In the northern part of the area, a splay may floor in this detachment fault zone, explaining the omission of the Triassic rocks.

4.2. Neogene Alpine Structures

[35] The number of reverse faults cutting the older Alpine structures varies from west to east (see geological map and cross sections, Figures 10, 11, and 12). These faults have an ENE-WSW strike and dips between 45° and 90° toward the NNW. The fault zone of these thrusts comprises uncohesive fault rocks: fault gouges and fault breccias and is thin (only several centimeters). The limits of the fault zone are sharp and the gouges contain brittle microfaults surfaces and cataclastic foliation. The striae within the microfault surfaces have trends varying between NW-SE and WNW-ESE, and the kinematic criteria (mainly brittle S-C structures) indicate a top-to-the-SE and -ESE sense of movement (Figure 13). The faults usually have a net slip with a strong right-lateral strike-slip component. The displacement of these reverse and right-lateral reverse faults varies between hundreds of meters and kilometers. The faults cut the Ciudad Granada Formation (early-middle Aquitanian), while, in map view, the Fuente-Espejos Formation (early Burdigalian to lower part of the late Burdigalian) overlies the different splays, suggesting a late Aquitanian age for the movement of these structures.

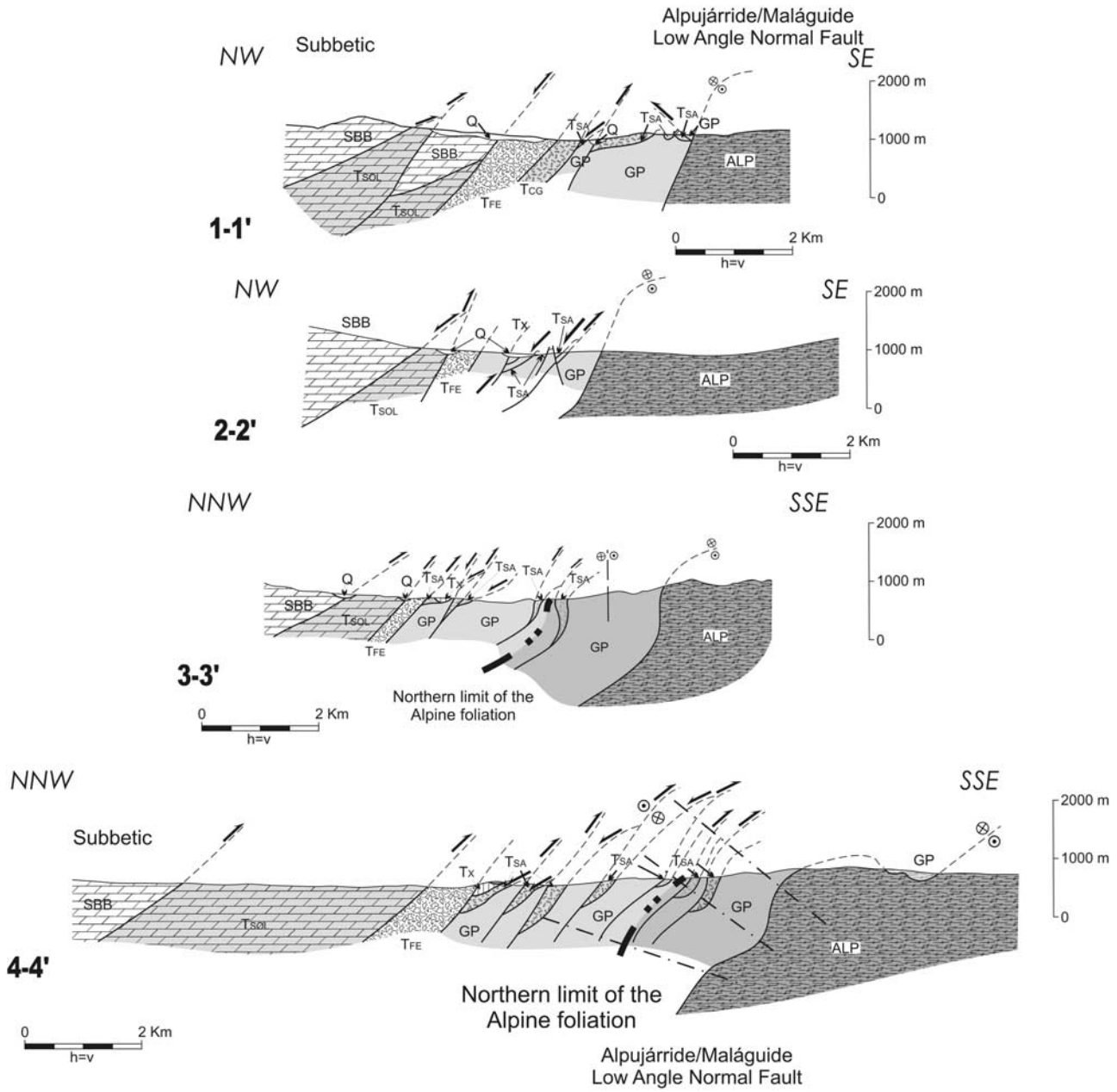

Figure 12. Cross sections of the Maláguide Complex. See Figures 9 and 10 for location. Legend is the same as in Figures 10 and 11.

[36] The basal contact of the Maláguide Complex is a low-angle normal fault that separates it from the underlying Alpujárride Complex [*Aldaya et al.*, 1991; *Lonergan and Platt*, 1995]. The fault surface has a ENE-WSW strike and a subvertical dip in the central and western part of the study area. This fault surface is folded by an ENE-WSW antiform with NNW vergence. In the study area, it is mainly the subvertical limb of the fold that crops out, accounting for the large dips of the fault surfaces. The hinge of the fold outcrops in the eastern end of the area (Figures 11 and 12) where the fault surfaces become subhorizontal and outcrops in a small tectonic window.

[37] The fault has brittle uncohesive fault rocks around a meter thick with gray fault gouges derived from metapelites and yellow carbonatic fault gouges and breccias containing some gypsum bodies. The striae and kinematic criteria (S-C structures, cataclastic foliations and crushed tails of clasts, etc.) indicate a top-to-the-ENE sense of movement [*Aldaya et al.*, 1991]. In the hanging wall, there are small shear zones affecting the slaty cleavage in the pelites of the Saladilla Formation, also indicating a top-to-the-ENE sense of movement (Figure 15). In the footwall, *Lonergan and Platt* [1995] describe a carbonatic milonite 5 to 20 m thick that developed near the top of the Alpujárride rocks, but

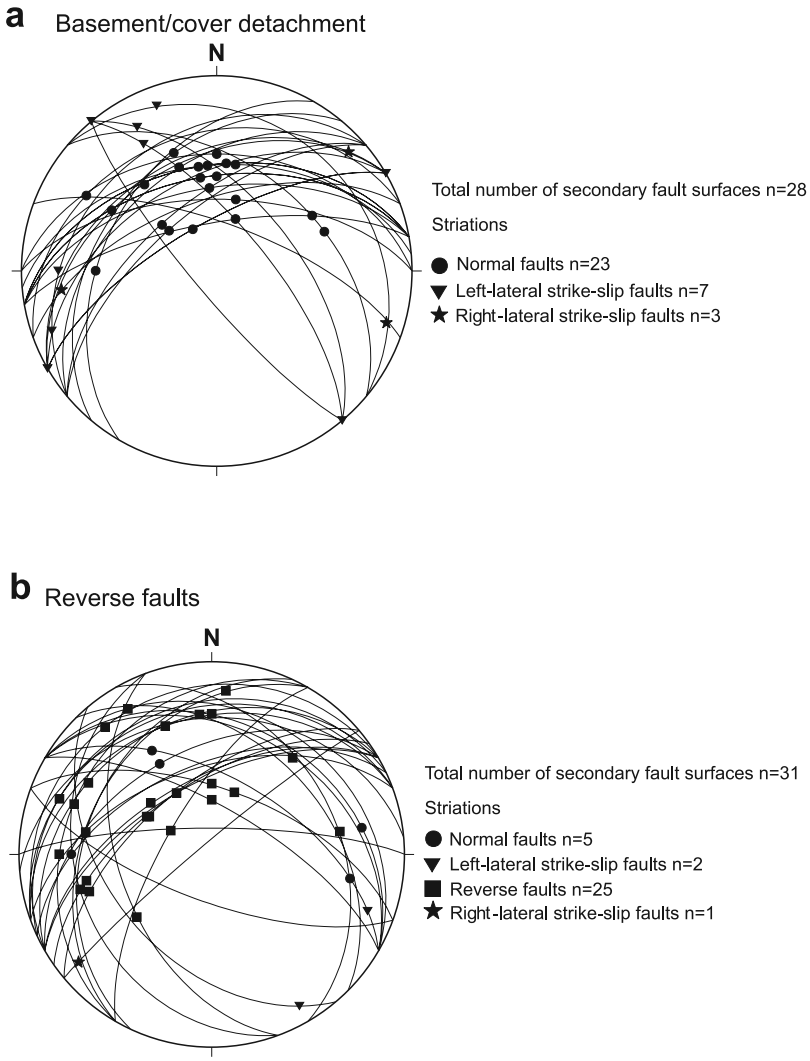

Figure 13. Stereograms with the orientation of the minor fault surfaces and slickenlines developed within the fault zone rocks in the Maláguide Complex (a) within the basement/cover detachment and (b) within the left-lateral reverse faults.

similar ductile fault rocks are not found in the hanging wall. The stretching lineation and kinematic criteria also confirm an ENE sense of movement of the hanging wall [*Lonergan and Platt*, 1995].

[38] If we unfold the ENE-WSW antiform and we put the Fuente-Espejos Formation in a horizontal position, the fault at the Maláguide/Alpujárride contact becomes a low-angle normal fault. The distances between the bottom of the Fuentes-Espejos Formation of the fault surface increase toward the east and, also, the fault surface has low-angle dips toward the east. The angle of dip can be deduced from the obliquity of the fault with the front of the Alpine slaty cleavage in the Maláguide Complex (around 20° of obliquity, Figure 11). The fault striation is approximately parallel to the line of maximum dip of the fault and the sense of movement is normal. This extensional character of the fault agrees with the decrease in the number of reverse faults toward the west (8 in the eastern study area and 2 in the western). The normal fault also explains the omission of the foliated rocks of the Saladilla Formation in the center and western part of the area. Moreover, the extensional character of this fault accounts for the superposition of both brittle fault rocks (pelitic and carbonatic fault gouges) in the hanging wall over ductile fault rocks (carbonate milonites) in the footwall.

[39] The second set of ENE-WSW striae that developed in the detachment between the Paleozoic basement and the Mesozoic-Cenozoic cover of the Maláguide Complex is subparallel to the striation in the Maláguide/Alpujárride contact, which suggests that the surface of the basement/cover detachment was reactivated during the movement of the Maláguide/Alpujárride contact and accommodate part of the internal extension of the hanging wall.

[40] The Blanquizares-Oria unit of the Alpujárride Complex crops out in the footwall of this low-angle normal fault [*Akkerman et al.*, 1980]. In this unit, Mg-rich chlorite

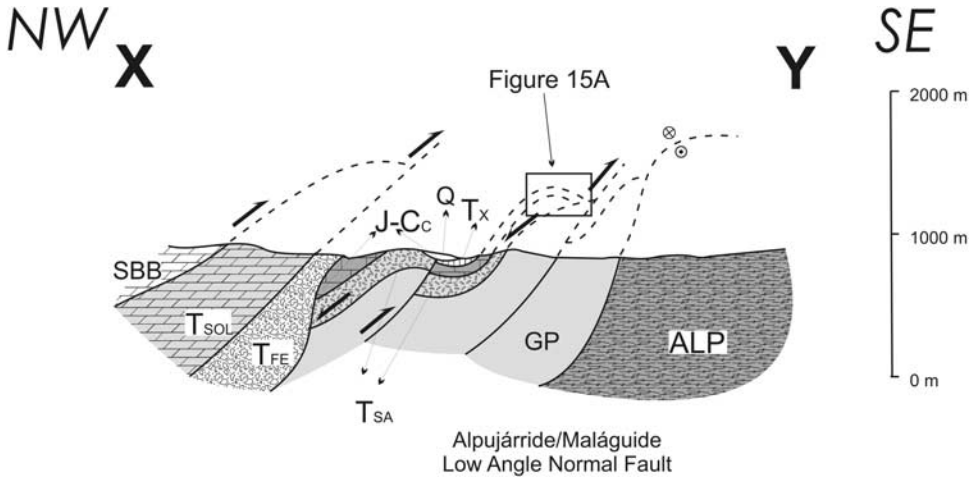

Figure 14. Cross section of the Maláguide Complex near the Vélez Rubio Village. See Figure 9 for location. The cross section illustrates the thinning of the Triassic rocks of the Saladilla Formation. Legend is the same as in Figures 10 and 11.

pseudomorphs the carpholite in quartz veins without chloritoid, indicating minimum pressures of 6–7 kbar and temperatures around 280–300°C [*Goffé et al.*, 1989, *Martínez-Martínez and Azañón*, 1997]. Also in Sierra Tercia, *Booth Rea* [2001] reported 300°C and 5.5 kbar of pressure for the Alpujárride rocks directly below the Maláguide Complex.

[41] The cooling ages determined by fission tracks in zircons and apatites in the Maláguide rocks (hanging wall) in this area are 240–307 Ma in the zircons and 23–18 Ma in apatites [*Johnson*, 1993; *Platt et al.*, 2005], whereas the ages determined in the Alpujárride Complex rocks (footwall) are the same for both zircons and apatites at around 18 Ma [*Johnson*, 1993; *Platt et al.*, 2005]. These ages suggest that the cooling of the Alpujárride rocks below the temperatures ranging between 330°C and the 120°C was very quickly indicating very high exhumation rates. These rates cannot be explained by strong erosion at 18 Ma because the Fuente-Espejos Formation (early Burdigalian to lower part of the late Burdigalian) was depositing at the same time. Consequently, we propose, in agreement with *Lonergan and Platt* [1995] and *Platt et al.* [2005], that this cooling was the consequence of the movement of the low-angle normal fault developed in the Maláguide/Alpujárride Complex. Moreover, if we suppose that the extension predates the cooling and therefore is anterior to the 23–18 Ma, as the reverse faults that have a late Aquitanian age, are also omitted by the low-angle normal fault, then this low-angle normal fault should be active in the early Burdigalian times. Both hypotheses coincide to date the extensional detachment at the Maláguide/Alpujárride contact at a narrow time interval between 20 and 18 Ma.

5. Discussion

[42] The oldest Alpine structures are the slaty cleavage associated with north vergent folds, the basaltic dikes, and the extensional detachment with a top-to-the-NNW sense of

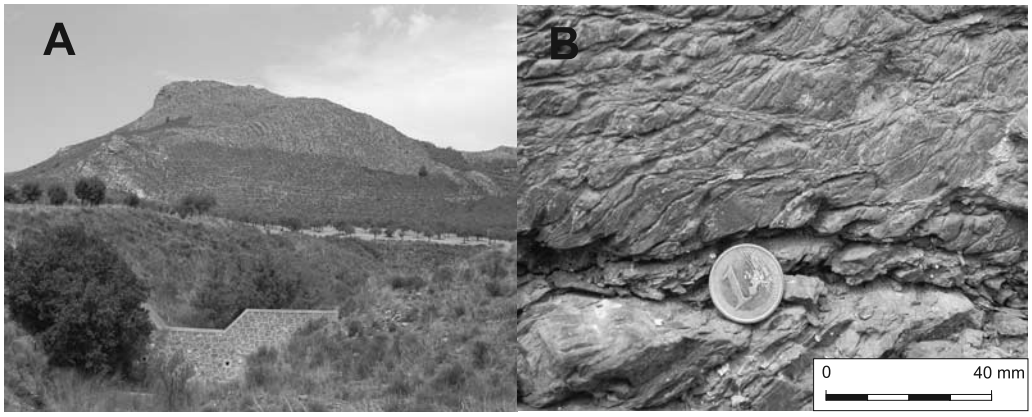

Figure 15. (a) View of the open anticline developed west of Velez Rubio village. See center of the cross section XY in Figure 10 and Figure 14 for location. (b) Small shear zones deforming the slaty cleavage in the Middle-Upper Triassic Saladilla Formation near the Maláguide/Alpujárride low-angle normal fault. East is located to the right of the photography.

movement. These structures were Eocene-Oligocene in age and can be correlated with similar structures described in the sector of Sierra Espuña and Sierra Tercia [*Lonergan*, 1991; *Nieto et al.*, 1994; *Lonergan and Platt*, 1995; *Booth Rea et al.*, 2002] and in the region near Málaga [*Torres-Roldán et al.*, 1986]. The foliation formed in anchizone conditions, as did those described in Sierra Espuña and Sierra Tercia [*Lonergan*, 1991; *Nieto et al.*, 1994; *Lonergan and Platt*, 1995; *Booth Rea et al.*, 2002]. Temperatures reached 270°C–300°C, conditions that agree with those determined by *Booth Rea* [2001] in Sierra Tercia. Moreover, a similar retrograde stage has been determined in Sierra Espuña [*Nieto et al.*, 1994].

[43] According to *Lonergan* [1993], the slaty cleavage can be correlated with the Eocene-Oligocene thrust stack that developed within the Maláguide Complex. This thrust stack is well preserved in the Sierra Espuña area, 22 km to the northeast of the study area (Figure 2) [*Paquet*, 1969; *Lonergan*, 1993], but cannot be recognized within the Sierra Tercia and Vélez Rubio areas. However, there must have been a thrust stack to provide the anchizone conditions determined in the eastern Maláguide rocks of the study area (Figure 11). This thrust stack also had to have developed on top of the Alpujárride rocks that have undergone a metamorphism with pressure conditions near 7 kbar while the temperatures were around 300°C in this area [*Martínez-Martínez and Azañón*, 1997]. These temperature conditions are not very different from the anchizone conditions reached in the foliated Triassic rocks of the Maláguide Complex during the Eocene associated with ductile deformations [*Platt et al.*, 2005, 2006]. Therefore the Maláguide Complex may represent the upper part of the orogenic wedge providing the load for the metamorphism in the Alpujárride as the cold metamorphism described here can be found only in thickened crust.

[44] The compression accommodated by this thrust stack during the Eocene-Oligocene may be correlated with the compressional stage recorded in the Iberian Peninsula that corresponded to the convergence between Iberia and Europe with the formation of the Pyrenees, Basque-Cantabrian mountain chain, Catalan Coastal Ranges and Iberian Chain (see *Jabaloy et al.* [2003, and references therein] for a summary of the deformations and paleostresses during this compressive stage). A similar compressional stage corresponds to the formation of the Alps and their prolongation trough Corsica [e.g., *Jolivet and Facenna*, 2000]. The ancient Alpine structures of the Maláguide, although fragmentary, suggest that the Maláguide represents the upper part of an accretionary wedge of units that undergone HP/LT metamorphism in the Eocene. These rocks, together with the Alpujárride Complex, resemble similar allochthonous metamorphic complexes in the Rif, Tell and Calabro-Peloritan belts and were usually interpreted as part of the same orogenic belt [*Michard et al.*, 2006]. However, the paleogeographic position and relationship with the rest of the elements (Iberia, Apulia, Europe, and the Alps) is controversial and two main hypothesis are proposed: (1) the orogen was an isolated block within the Tethys ocean [*Bouillin et al.*, 1986; *Doglioni*, 1992; *Guerrera et al.*, 1993, 2005], and (2) the orogen was continuous with the Alps and developed in the margin of Iberia and Sardinia [*Doglioni et al.*, 1997, 1999; *Michard et al.*, 2006].

[45] The swarm of basaltic dikes is attributed to the late Eocene-Basal Oligocene, according to the ages determined by *Turner et al.* [1999] and *Duggen et al.* [2004]. Assuming this age, the slaty cleavage must be older, and we can propose a middle Eocene age for the development of this structure. This attribution agrees with the lower Eocene proposal (around 48 Ma) by *Platt et al.* [2005] for the age of the main foliation on the Blanquizares-Oria unit and other Alpujárride units.

[46] The basalt within the dikes has island arc tholeiitic affinities and is intruded into continental crust. In order to produce tholeiitic basalts, the upper mantle has to be affected by partial melting in conditions of relatively low pressure. This mantle must be enriched in several elements that are more frequent in continental crust [*Turner et al.*, 1999]. The most common mechanism producing such mantle contamination is the subduction of sediments located on oceanic crust. *Duggen et al.* [2004] use this mechanism to explain the chemistry of the dikes and their relative enrichment in fluid-mobile elements as currently occurs in the back-arc environments (island arc tholeiites) of the Izu Bonin and South Sandwich island arcs. Finding this dike swarm in the Vélez Rubio region means the swarm extends some 300 km, from Fuengirola to Vélez Rubio. This band is 10 to 20 km broad with an ENE-WSW trend and may correspond to the location of an old volcanic front in a back-arc environment during the late Eocene.

[47] Modern oceanic mantle melts as the MORB and OIB have low Th/La ratios, normally lower than 0.1, and the intraplate volcanism have normally Th/La values lower than 0.2, while high values for this ratio is a signature of the continental crust and the sediments derived from it [*Plank*, 2005]. In subducting sediments the Th/La varies in function of the quantities of terrigenous material derived from the continental crust (high Th/La ratios), the quantities of fish debris phosphate and hydrogenous Fe-Mn oxides (low Th/La ratios), and the quantities of volcanoclastic derived material (usually with low Th/La ratios as normally they are MORB and BIO rocks). Therefore different sediments have different Th/La and produce a distinctive a signal. When this sediment is subducted, this signal can be looked for in the volcanic arc rocks. The result is that there is little change in Th/La ratios from the subducting sediments to the lavas erupting in the volcanic arc [*Plank*, 2005]. The high Th/La ratio in the basaltic dikes in the Vélez Rubio and Málaga area indicates that the upper mantle contamination has a signal from the upper continental crust: or upper crustal continental rocks subducting directly in the mantle or terrigenous sediments with little mixing from the phosphate/hydrogenous Fe-Mn and volcanoclastic components. This signal may help to identify the rocks entering in the upper mantle.

[48] The other ancient Alpine structure is the fault zone (top-to-the-NNW sense of movement) that separates the Paleozoic basement from the cover. We interpret this fault zone, imbricated by the Aquitanian reverse faults, as an

extensional detachment due to the omission of the Triassic and Jurassic formations in the hanging wall of the fault zone. This fault zone is capped by the Ciudad Granada Formation (early-middle Aquitanian [*González Donoso et al.*, 1988]), indicating that the zone is pre-Aquitanian and probably Oligocene (Figures 10, 11, 12, and 14). We have not directly observed the relationships between this fault zone and the slaty cleavage. However, the different conditions recorded by both structures (namely, the ductile deformation recorded by the slaty cleavage and the near to the surface conditions marked by the uncohesive fault rocks of the extensional detachment, as well as the aforementioned attributions of the ages of these structures, although very indirect) allow us to assume in this work that the slaty cleavage is the oldest Alpine structure in the Maláguide Complex.

[49] This detachment may also explain the absence of the Eocene-Oligocene thrusts with top-to-the-NNW sense of movement described in the area of Sierra Espuña, and the lack of a very thick succession of rocks that could explain the anchizone conditions necessary for the development of the slaty cleavage. Furthermore, the parallelism between the direction and sense of movement of the extensional detachment and the Eocene-Oligocene thrust system suggests that the two structures are related; one possible explanation is that the orogenic wedge formed by the Maláguide/Alpujárride collapsed and produced the extensional structures. In the Alpujárride Complex, spectacular low-angle normal faults with a NNW-SSE extension thin the whole complex [e.g., *Crespo-Blanc et al.*, 1994; *Crespo-Blanc*, 1995; *Azañón and Crespo-Blanc*, 2000; *Rossetti et al.*, 2005] but have been normally attributed to the Burdigalian-Langhian times [*Crespo-Blanc et al.*, 1994]. However, more recently, *Rossetti et al.* [2005] interpret that this NNW-SSE extension begun in the Aquitanian, suggesting that all the NNW-SSE extensional structures can be the product of an unique stage.

[50] These Paleogene structures help to constrain the evolution of the Internal Zones during this period. The deformation began with the formation of the slaty cleavage associated with north vergent structures during the middle Eocene on top of the Alpujárride rocks that underwent MP/LT metamorphism in this area. In the late Eocene–early Oligocene, the rocks were intruded by arc-island tholeiitic basalts, suggesting a back-arc environment of these rocks at this moment. The thrust stack necessary to provide the temperature conditions is not preserved in the study area and may have been omitted by the detachment fault (probably Oligocene) separating the basement and the cover with a top-to-the-NNW sense of movement. All these deformations can be correlated with a major deformation event prior to the convergence between the External and the Internal Zones.

[51] In addition to the structures that developed during the Paleogene in the Maláguide Complex, there are several structures with early Miocene ages that we can associate directly with the convergence between the Internal and the External Zones (Figure 16). These structures are the reverse faults and the low-angle normal fault separating the Maláguide from the Alpujárride Complex.

[52] The reverse faults, with an ESE sense of movement of the hanging wall, have a late Aquitanian age, and therefore predate the thrusting of the Subbetic and the Solana Formation over the Internal Zones [*Lonergan*, 1993; *Fernández-Fernández et al.*, 2004] (Figure 16), indicating that in this area the sequence of thrusts began in the Internal Zones. The reverse faults have a large, right-lateral strike-slip component of the displacement and recorded right-lateral transpression, as did the regime proposed for the convergence between the Internal and the External Zones during the early Miocene [*Lonergan and White*, 1997; *Fernández-Fernández et al.*, 2004]. Migration of the deformation toward the External Zones occurred during the early-middle Burdigalian with the folding of the Subbetic rocks, their vertical axis rotations, and the thrusting [*Fernández-Fernández et al.*, 2004].

[53] The reverse faults of the Maláguide Complex are unconformably covered by the Fuente-Espejos Formation, which records the subsidence of the Maláguide Complex during the Burdigalian. The subsidence was accompanied by the deposition of the olistostromes and clasts from the thrust front of the Subbetic and the Solana Formation. Additionally, clasts from the Alpujárride Complex were deposited, indicating that this complex reached the surface during this period. These deposits suggest a Burdigalian age for the movement of the low-angle normal fault that now separates the two complexes. We have discussed previously the age of this fault based on fission track studies [*Johnson*, 1993; *Platt et al.*, 2005] and the age of the reverse faults. This age is restricted to the interval between 20 and 18 Ma. This Burdigalian age for the movement of the low-angle normal fault helps to explain the subsidence of the Maláguide Complex during this period. However, the most important thing is that with these ages both the compressive structures in the Subbetic and the Solana Formation and the extensional structures producing the exhumation of the HP/LT Alpujárride rocks are contemporaneous. Both deformations indicate that the NW-SE shortening that accommodated the convergence of the External and Internal Zones was accompanied by NE-SW extension, probably due to the lateral extrusion of the rocks of the Internal Zones (Figure 16). The reverse faults and the thrusting of the Subbetic over the Maláguide seem to be back-thrust structures in the whole structure of the orogen that mainly have a NW vergence and facing of the structures.

[54] The Internal Zones have been interpreted as the rigid back stop of the orogenic wedge of the External Zones during the Neogene. However, current data indicate that the hinterland of the orogen was not rigid, instead reacting by extending and thinning approximately perpendicular to the shortening. This convergence between the Internal and the External Zones are equivalent to the collision of the Internal Zones of the Rif against the North African margin, the Kabylian metamorphic allochthonous terrain over the External Tell and the development of the western Mediterranean oceanic basins in a back-arc location [*Lacombe and Jolivet*, 2005; *Michard et al.*, 2006]. Another alternative model is proposed by *Doglioni et al.* [1997, 1998, 1999]; in this model the extension affecting the Betics was the effect

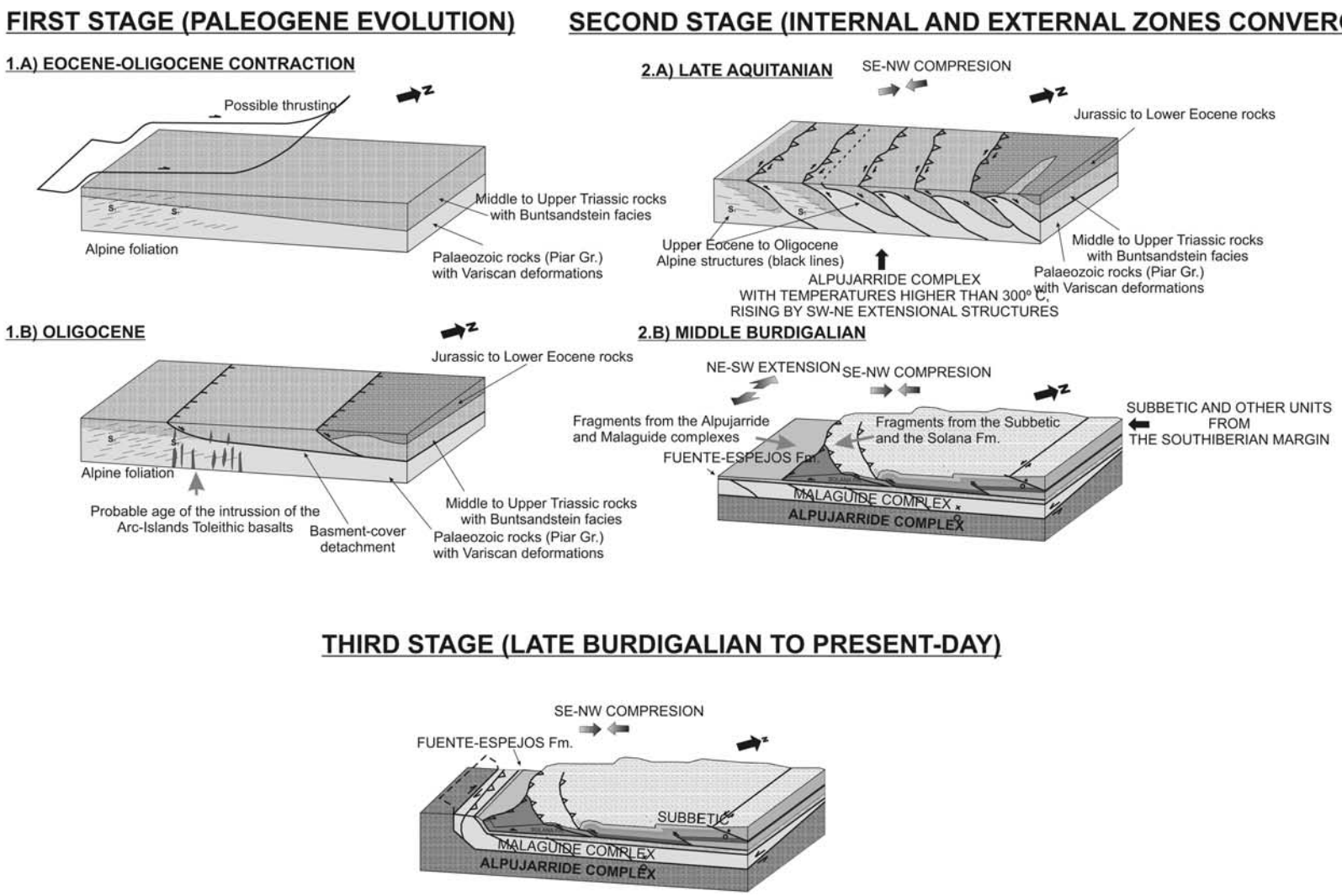

Figure 16. Sketch illustrating the proposed evolution of the Malaguide Complex rocks during the Alpine orogeny with the three main stages. Stage 1, the Paleogene evolution prior to the Internal and External Zones convergence; stage 2, the Aquitanian-middle Burdigalian stage that records the Internal-External Zones convergence; and stage 3, the late Burdigalian to present-day stage when both zones were welded.

of back-arc extension of the Apennines-Maghrebides subduction. They propose that normal faults obliquely overlapped the compression in the central and eastern Betics.

[55] The youngest structures include the formation of NE-SW folds (Figure 16) and the NW-SE normal faults of the Lorca Basin. The NE-SW folds verge northward and develop in both the External and in the Internal Zones, while the normal faults cut these folds and the External/Internal Zones boundary, indicating that the two zones have been welded from the middle Miocene to the Present.

6. Conclusions

[56] The Alpine deformations in the Maláguide Complex (Vélez Rubio area, Eastern Betic Cordillera) can be grouped into three main stages. The first comprises the Paleogene structures prior to the convergence of the Internal and External Zones. This main stage began with compressional deformation that produced a synmetamorphic slaty cleavage under anchizone conditions (270°C–300°C). This foliation is associated with northward vergent structures and was probably connected with the superposition of the Maláguide Complex over the Alpujárride during the middle Eocene. This structure is intruded by an island arc tholeiitic basaltic swarm. The Maláguide Complex was thinned, most likely during the Oligocene, by an extensional detachment with a NNW sense of movement of the hanging wall.

[57] The second stage consists of the convergence of the External and Internal Zones during the Aquitanian-Burdigalian. This convergence was a right-lateral transpression that produced structures with vergence toward the hinterland that superposed the External over the Internal Zones. The hinterland was not a rigid backstop and was deformed with compressional and extensional structures that produced the exhumation of the HP/LT rocks of the Alpujárride Complex.

[58] The third stage corresponds to the evolution from the late Burdigalian to the present-day, when the Internal and External Zones were welded and deformed in a NW-SE shortening direction parallel to the convergence trend between Africa and Europe and NE-SW extension.

[59] **Acknowledgments.** We would like to thank Carlo Doglioni, Giacomo Prosser, Guido Grosso, and Maria Iole Spalla for the revisions of the paper. Christine Laurin revised the English text. We would also like to thank Fernando Gervilla and Claudio Marchesi for their help with the geochemical data. This work was financed by the Spanish research project BTE2003-01699 from the CICYT and the Spanish research project CSD2006-00041 from the CONSOLIDER-INGENIO2010.

References

Akkerman, J. H., G. Maier, and O. J. Simon (1980), On the geology of the Alpujarride Complex in the western Sierra de las Estancias (Betic Cordilleras, SE Spain), *Geol. Mijnbouw*, *59*, 363–374.

Aldaya, F., F. Alvarez, J. Galindo-Zaldívar, F. González-Lodeiro, A. Jabaloy, and F. Navarro-Vilá (1991), The Maláguide-Alpujárride contact (Betic Cordilleras, Spain): A brittle extensional detachment, *C. R. Acad. Sci., Ser. II*, *313*(101), 1447–1453.

Azañón, J. M., and A. Crespo-Blanc (2000), Exhumation during a continental collision inferred from the tectonometamorphic evolution of the Alpujarride Complex in the central Betics (Alboran Domain, SE Spain), *Tectonics*, *19*, 549–565.

Balanyá, J. C. (1991), Estructura del Dominio de Alborán en la parte norte del Arco de Gibraltar, Ph.D. thesis, 210 pp., Univ. de Granada, Granada, Spain.

Balanyá, J. C., and V. García Dueñas (1987), Les directions structurales dans le Domaine d'Alborán de part et d'autre du Détroit de Gibraltar, *C. R. Acad. Sci., Ser. II*, *304*(15), 929–932.

Battaglia, S., L. Leoni, and F. Sartori (2003), Mineralogical and grain size composition of clays developing calanchi and biancane erosional landforms, *Geomorphology*, *49*(1–2), 153–170.

Bevins, R. E., D. Robinson, and G. Rowbotham (1989), Compositional variations in mafic phyllosilicates from regional low-grade metabasites and application of the chlorite geothermometer, *J. Metamorph. Geol.*, *9*(6), 711–721.

Blein, O., S. Guillot, H. Lapierre, B. Mercier de Lépinay, J. M. Lardeaux, G. Millan Trujillo, M. Campos, and A. Garcia (2003), Geochemistry of the Mabujina Complex, Central Cuba: Implications on the Cuban Cretaceous Arc Rocks, *J. Geol.*, *111*, 89–101.

Booth Rea, G. (2001), Tectónica Cenozoica en el Dominio de Alborán, Ph.D. thesis, 240 pp., Univ. de Granada, Granada, Spain.

Booth Rea, G., V. García-Dueñas, and J. M. Azañón (2002), Extensional attenuation of the Malaguide and Alpujarride thrust sheets in a segment of the Alboran Basin folded during the Tortonian (Lorca area, Eastern Betic), *C. R. Acad. Sci.*, *334*, 1–8.

Bouillin, J.-P., M. Durand-Delga, and P. Olivier (1986), Betic-Rifian and Tyrrhenian arcs: Distinctive features, genesis, and development stages, in *The Origin of Arcs* edited by F. C. Wezel, pp. 281–304, Elsevier, New York.

Crespo-Blanc, A. (1995), Interference of extensional fault systems: A case study of the Miocene rifting of the Alboran basement (north of Sierra Nevada, Betic Chain), *J. Struct. Geol.*, *17*, 1559–1569.

Crespo-Blanc, A., M. Orozco, and V. García-Dueñas (1994), Extension versus compression during the Miocene tectonic evolution of the Betic Chain: Late folding of normal fault systems, *Tectonics*, *13*, 78–88.

Doglioni, C. (1992), Main differences between thrust belts, *Terra Nova*, *4*(2), 152–164.

Doglioni, C., E. Gueguen, F. Sabat, and M. Fernandez (1997), The western Mediterranean extensional basins and the Alpine orogen, *Terra Nova*, *9*(3), 109–112.

Doglioni, C., M. Fernandez, E. Gueguen, and F. Sabat (1998), On the interference between the early Apennines-Maghrebides backarc extension and the Alps-Betics orogen in the Neogene geodynamics of the western Mediterranean, *Boll. Soc. Geol. Ital.*, *118*, 75–89.

Doglioni, C., E. Gueguen, P. Harabaglia, and F. Mongelli (1999), On the origin of W-directed subduction zones and applications to the western Mediterranean, *Geol. Soc. Spec. Publ.*, *156*, 541–561.

Duggen, S., K. Hoernle, P. van den Bogaard, and C. Harris (2004), Magmatic evolution of the Alboran region: The role of subduction in forming the western Mediterranean and causing the Messinian Salinity Crisis, *Earth Planet. Sci. Lett.*, *218*, 91–108, doi:10.1016/S0012-821X (03)00632-0.

Egeler, C. G., and O. J. Simon (1969), Orogenic evolution of the Betic zone (Betic cordilleras, Spain), with emphasis on the nappe structures, *Geol. Mijnbouw*, *48*, 296–305.

Fallot, P. (1948), Les Cordillères bétiques, *Estud. Geol.*, *IV*, 83–173.

Fernández-Fernández, E., A. Jabaloy, and F. González Lodeiro (2004), Lower Miocene deformation in the hanging wall of the Internal-External Zone boundary of the Betic Cordilleras: Deformation at the edges of vertical-axis rotation domains in oblique convergent margins, in *Vertical Coupling and Decoupling in the Lithosphere*, edited by J. Grocott et al., *Geol. Soc. Spec. Publ.*, *227*, 249–278.

Frey, M. (1987), The reaction-isograd kaolinite + quartz = pyrophyllite + H_2O, Helvetic Alps, Switzerland, *Schweiz. Mineral. Petrogr. Mitt.*, *67*(1–2), 1–11.

Galindo-Zaldívar, J., F. González-Lodeiro, and A. Jabaloy (1989), Progressive extensional shear structures in a detachment contact in the western Sierra Nevada (Betic Cordilleras, Spain), *Geodin. Acta*, *3*, 73–85.

Geel, T. (1973), The geology of the Betic of Malaga, the Subbetic and the zone between these two units in the Velez Rubio area (southern Spain), *GUA Pap. Geol. 5*, 191 pp., Stichting GUA, Geol. Inst., Amsterdam.

Geel, T., and T. B. Roep (1998), Oligocene to middle Miocene basin development in the Eastern Betic Cordilleras, SE Spain (Vélez Rubio Corridor–Espuña): Reflections of west Mediterranean plate-tectonic reorganizations, *Basin Res.*, *10*, 325–343.

Goffé, B., A. Michard, V. García-Dueñas, F. González-Lodeiro, P. Monié, J. Campos, J. Galindo-Zaldívar, A. Jabaloy, J. M. Martínez-Martínez, and F. Simancas (1989), First evidence of high-pressure, low-temperature metamorphism in the Alpujarride nappes, Betic Cordilleras (SE Spain), *Eur. J. Mineral.*, *1*, 139–142.

González Donoso, J. M., D. Linares, E. Molina, and F. Serrano (1988), El Mioceno inferior de Chirivel (Almería): Bioestratigrafía, cronoestratigrafía y significado tectosedimentario de las formaciones de Ciudad Granada y Fuente-Espejos, *Rev. Soc. Geol. Esp.*, *1*, 53–71.

González-Lodeiro, F., F. Aldaya, J. Galindo-Zaldívar, and A. Jabaloy (1996), Superposition of extensional detachments during the Neogene in the internal zones of the Betic Cordilleras, *Geol. Rundsch.*, *85*, 350–362.

Guerrera, F., A. Martín-Algarra, and V. Perrone (1993), Late Oligocene-Miocene syn-/-late-orogenic successions in western and central Mediterranean

Chains from the Betic Cordillera to the southern Apennines, *Terra Nova*, *5*, 525–544.

Guerrera, F., M. Martín-Martín, V. Perrone, and M. Tramontana (2005), Tectono-sedimentary evolution of the southern branch of the western Tethys (Maghrebian Flysch basin and Lucanian Ocean): Consequences for western Mediterranean geodynamics, *Terra Nova*, *17*, 358–367.

Hermes, J. J. (1977), Remarks on the middle Eocene to Miocene sequence of Sierra de la Puerta (south Prebetic) near Caravaca, southern Spain, *Proc. K. Ned. Akad. Wet.*, *80*(2), 100–105.

Jabaloy, A., J. Galindo-Zaldívar, and F. González Lodeiro (1993), The Alpujárride Nevado-Filabride extensional shear zone, Betic-Cordilleras, SE Spain, *J. Struct. Geol.*, *15*(3–5), 555–569.

Jabaloy, A., J. Galindo-Zaldívar, and F. González-Lodeiro (2003), Palaeostress evolution of the Iberian Peninsula (Late Carboniferous to present-day), *Tectonophysics*, *357*, 159–186.

Jabaloy-Sánchez, A., E. M. Fernández-Fernández, and F. González-Lodeiro (2007), The structure of the eastern Betic Cordillera (SE Spain) according to a seismic reflection profile, *Tectonophysics*, *433*, 97–126, doi:10.1016/j.tecto.2006.11.004.

Johnson, C. (1993), Contrasted thermal histories of different nappe complexes in SE Spain: Evidence for complex crustal extension: Late orogenic extension, in *Late Orogenic Extension in Mountain Belt*, edited by M. Séranne and J. Malavieille, *Doc. B.R.G.M.*, *219*, 103.

Jolivet, L., and C. Facenna (2000), Mediterranean extension and the Africa-Eurasia collision, *Tectonics*, *19*, 1095–1106.

Kirker, A. I., and J. P. Platt (1998), Unidirectional slip vector in the western Betic Cordilleras: Implications for the formation of the Gibraltar arc, *J. Geol. Soc. London*, *155*, 193–207.

Kisch, H. J. (1989), Discordant relationships between degree of very low grade metamorphism and the development of slaty cleavage, in *Evolution of Metamorphic Belts*, edited by J. S. Daly, R. A. Cliff, and B. W. D. Yardley, *Geol. Soc. Spec. Publ.*, *43*, 173–175.

Kisch, H. J. (1991a), Development of slaty cleavage and degree of very-low-grade metamorphism; a review, *J. Metamorph. Geol.*, *9*(6), 735–750.

Kisch, H. J. (1991b), Illite crystallinity: Recommendations on sample preparation, X-ray diffraction settings, and interlaboratory samples, *J. Metamorph. Geol.*, *9*(6), 665–670.

Kozur, H., C. W. H. Mulder-Blanken, and O. J. Simon (1985), On the Triassic of the Betic Cordilleras (S. Spain), with special emphasis on holothurian sclerites, *Proc. K. Ned. Akad. Wet., Ser. B*, *88*, 83–110.

Lacombe, O., and L. Jolivet (2005), Structural and kinematic relationships between Corsica and the Pyrenees-Provence domain at the time of the Pyrenean orogeny, *Tectonics*, *24*, TC1003, doi:10.1029/2004TC001673.

Le Bas, M. J., R. W. Le Maitre, A. Streckseisen, and B. Zanetti (1986), A chemical classification of volcanic rocks based on total alkali-silica diagram, *J. Petrol.*, *27*, 745–754.

Lonergan, L. (1991), Structural evolution of the Sierra Espuña, Betic Cordillera, SE Spain, Ph.D. thesis, 154 pp., Univ. of Oxford, Oxford, U.K.

Lonergan, L. (1993), Timing and kinematics of deformation in the Malaguide Complex, Internal Zone of the Betic Cordillera, southeast Spain, *Tectonics*, *12*, 460–476.

Lonergan, L., and J. P. Platt (1995), The Malagide-Alpujarride boundary: A major extensional contact in the Internal Zone of the eastern Betic Cordillera, SE Spain, *J. Structural Geology*, *17*(12), 1655–1671.

Lonergan, L., and N. White (1997), Origin of the Betic-Rif mountain belt, *Tectonics*, *16*, 504–522.

López-Sánchez-Vizcaíno, V. L., D. Rubatto, M. T. Gómez-Pugnaire, V. Trommsdorff, and O. Müntener (2001), Middle Miocene high-pressure metamorphism and fast exhumation of the Nevado-Filábride Complex: SE Spain, *Terra Nova*, *13*, 327–332, doi:10.1046/j.1365-3121.2001.00354.x.

Mac Gillavry, H. J., T. Geel, T. B. Roep, and H. Soediono (1963), Further notes on the geology of the Betic of Malaga, the Subbetic, and the zone between these two units, in the region of Velez Rubio (southern Spain), *Geol. Rundsch.*, *53*, 233–256.

Mäkel, G. H. (1985). The geology of the Malaguide Complex and its bearing on the geodynamic evolution of the Betic-Rif Orogen (southern Spain and northern Morocco), *>GUA Pap. Geol. 22*, 263 pp., Stichting GUA, Geol. Inst., Amsterdam.

Mäkel, G. H., and H. E. Rondeel (1979), Differences in the stratigraphy and metamorphism between superposed Maláguide and Alpujárride units in the Espuña area (Betic Cordilleras, SE Spain), *Estud. Geol.*, *35*, 109–117.

Martín-Algarra, A. (1987), Evolución geológica alpina del contacto entre las Zonas Internas y las Zonas Externas de las Cordilleras Béticas, Ph.D. thesis, 1171 pp., Univ. of Granada, Granada, Spain.

Martín-Martín, M., B. El Mamoune, A. Martín-Algarra, and J.A. Marín-Pérez (1996), The Internal-External Zone boundary in the eastern Betic Cordillera, SE Spain: Discussion, *J. Struct. Geol.*, *18*, 523–524.

Martínez-Martínez, J. M., and J.-M. Azañón (1997), Modes of extensional tectonics in the southeastern Betics (SE Spain): Implications for the tectonic evolution of the peri-Alborán orogenic system, *Tectonics*, *16*, 205–225.

Michard, A., F. Negro, O. Saddiqi, M. L. Bouybaouene, A. Chalouan, R. Montigny, and B. Goffé (2006), Pressure-temperature-time constraints on the Maghrebide mountain building: Evidence from the Rif-Betic transect (Morocco, Spain), Algerian correlations, and geodynamic implications, *C. R. Geosci.*, *338*, 92–114.

Nebbad, F. (2001), Le prisme orogenique Prebétique (Sud-Est de l'Espagne), Évolution cinématique et coupes equilibrées, Ph.D. thesis, 239 pp., Univ. of Orsay Paris XI, Orsay, France.

Nieto, F., and A. Sánchez-Navas (1994), A comparative XRD and TEM study of the physical meaning of the white mica ''crystallinity'' index, *Eur. J. Mineral.*, *6*(5), 611–621.

Nieto, F., N. Velilla, D. R. Peacor, and M. Ortega-Huertas (1994), Regional retrograde alteration of subgreenschist facies chlorite to smectite, *Contrib. Mineral. Petrol.*, *115*, 243–252.

Nieto, F., M.-P. Mata, B. Bauluz, G. Giorgetti, P. Arkai, and D. R. Peacor (2005), Retrograde diagenesis, a widespread process on a regional scale, *Clay Miner.*, *40*(1), 93–104, doi:10.1180/0009855054010158.

Paquet, J. (1969), Étude geologique de l'ouest de la Province de Murcie (Espagne), *Mem. Soc. Geol. Fr.*, *3*, 270 pp.

Pearce, J. A., and J. R. Cann (1973), Tectonic setting of basic volcanic rocks determined using trace elements analyses, *Earth Planet. Sci. Lett.*, *19*, 290–300.

Plank, T. (2005), Constraints from thorium/lanthanum on sediment recycling at subduction zones and the evolution of the continents, *J. Petrol.*, *46*, 921–944.

Platt, J. P., S. P. Kelley, A. Carter, and M. Orozco (2005), Timing of tectonic events in the Alpujarride Complex, Betic Cordillera, southern Spain, *J. Geol. Soc. London*, *162*, 451–462.

Platt, J. P., R. Anczkiewicz, J.-I. Soto, S. P. Kelley, and M. Thirlwall (2006), Early Miocene continental subduction and rapid exhumation in the western Mediterranean, *Geology*, *34*(11), 981–984, doi:10.1130/G22801A.1.

Rossetti, F., C. Faccenna, and A. Crespo-Blanc (2005), Structural and kinematic constraints to the exhumation of the Alpujarride Complex (central Betic Cordillera, Spain), *J. Struct. Geol.*, *27*, 199–216, doi:10.1016/j.jsg.2004.10.008.

Simon, O. J., and H. Visscher (1983), El Pérmico de las Cordilleras Béticas, in *Carbonífero y Pérmico de España*, *Actas X Congr. Int. Estrat. Geol. Carbonifero*, edited by C. Martínez-Díaz, pp. 453–499, Inst. Geol. y Minero de España, Madrid.

Snoke, A. W., and J. Tullis (1998), An overview of fault rocks, in *Fault-Related Rocks. A Photographic Atlas*, edited by A. W. Snoke, J. Tullis, and V. R. Todd, pp. 3–18, Princeton Univ. Press, Princeton, N. J.

Soediono, H. (1971), Geological investigations in the Chirivel area, province of Almeria, southeastern Spain, Ph.D. thesis, 144 pp., Univ. of Amsterdam, Amsterdam.

Torres-Roldán, R. L., G. Poli, and A. Peccerillo (1986), An Early Miocene arc-tholeiitic magmatic dike event from the Alboran Sea: Evidence for precollisional subduction and back-arc crustal extension in the westernmost Mediterranean, *Geol. Rundsch.*, *75*, 219–234.

Turner, S. P., J. P. Platt, R. M. M. George, S. P. Kelley, D. G. Pearson, and M. G. Nowell (1999), Magmatism associated with orogenic collapse of the Betic-Alboran Domain, SE Spain, *J. Petrol.*, *40*(6), 1011–1036.

Warr, L. N., and A. H. N. Rice (1994), Interlaboratory standardization and calibration of clay mineral crystallinity and crystallite size data, *J. Metamorph. Geol.*, *12*, 141–152.

Wood, D. A. (1980), The application of a Th-Hf-Ta diagram to problems of tectonomagmatic classification and to establishing the nature of crustal contamination of basaltic lavas of the British Tertiary volcanic province, *Earth Planet. Sci. Lett.*, *50*, 11–30.

E. M. Fernández-Fernández, F. González-Lodeiro, and A. Jabaloy-Sánchez, Departamento de Geodinámica, Universidad de Granada, E-18071 Granada, Spain. (emferfer@inicia.es; jabaloy@ugr.es)

F. Nieto, Departamento de Mineralogía y Petrología, Universidad de Granada, 18071 Granada, Spain.